33. Perez F, Franchi M, Peli J. Effect of calcium hydroxide form and placement on root dentine pH. Int Endod J 2001: **34**: 417–423.
34. Pieringer RA. The metabolism of glyceride glycolipids. I. Biosynthesis of monoglucosyl diglyceride and diglucosyl diglyceride by glucosyltransferase pathways in *Streptococcus faecalis*. J Biol Chem 1968: **243**: 4894–4903.
35. Pinheiro ET, Gomes BP, Ferraz CC, Sousa EL, Teixeira FB, Souza-Filho FJ. Microorganisms from canals of root-filled teeth with periapical lesions. Int Endod J 2003: **36**: 1–11.
36. Rich RL, Kreikemeyer B, Owens RT et al. Ace is a collagen-binding MSCRAMM from *Enterococcus faecalis*. J Biol Chem 1999: **274**: 26939–26945.
37. Sato Y, Okamoto K, Kagami A, Yamamoto Y, Igarashi T, Kizaki H. *Streptococcus mutans* strains harboring collagen-binding adhesin. J Dent Res 2004: **83**: 534–539.
38. Sansone C, Van Houte J, Joshipura K, Kent R, Margolis HC. The association of mutans streptococci and non-mutans streptococci capable of acidogenesis at a low pH with dental caries on enamel and root surfaces. J Dent Res 1993: **72**: 508–516.
39. Sherman JM. The streptococci. Bacteriol Rev 1937: **1**: 3–97.
40. Siqueira JF, Uzeda M. Disinfection by calcium hydroxide paste of dentinal tubules infected with two obligate and one facultative anaerobic bacteria. J Endod 1996: **22**: 674–676.
41. Siren E, Haapasalo M, Ranta K, Salmi P, Kerosuo E. Microbiological findings and clinical treatment procedures in endodontic cases selected for microbiological investigation. Int Endod J 1997: **30**: 91–95.
42. Sjögren U, Figdor D, Spångberg L, Sundqvist G, The antimicrobial effect of calcium hydroxide as a short-term intracanal dressing. Int Endod J 1991: **24**: 119–125.
43. Sundqvist G, Figdor D, Persson S, Sjögren U. Microbiologic analysis of teeth with failed endodontic treatment and the outcome of conservative re-treatment. Oral Surg Oral Med Oral Pathol Oral Radiol Endod 1998: **85**: 86–93.
44. Switalski LM, Patti JM, Butcher W, Gristina AG, Speziale P, Hook M. A collagen receptor on *Staphylococcus aureus* strains isolated from patients with septic arthritis mediates adhesion to cartilage. Mol Microbiol 1993: **7**: 99–107.
45. Tamesada M, Kawabata S, Fujiwara T, Hamada S. Synergistic effects of streptococcal glucosyltransferases on adhesive biofilm formation. J Dent Res 2004: **83**: 874–879.
46. Tsujimoto K, Semadani M, Huflejt M, Packer L. Intracellular pH of halobacteria can be determined by the fluorescent dye 2′,7′-bis (carboxyethyl)-5(6)-carboxyfluorecein. Biochem Biophys Res Commun 1988: **155**: 123–129.
47. Winkler KC, Amerongen JV. Bacteriologic results from 4,000 root canal cultures. Oral Surg Oral Med Oral Pathol 1959: **12**: 857–875.

*Oral Microbiology Immunology 2006: 21: 201–205*
*Printed in Singapore. All rights reserved*



ORAL MICROBIOLOGY AND IMMUNOLOGY

# Difference in the xylitol sensitivity of acid production among *Streptococcus mutans* strains and the biochemical mechanism

**H. Miyasawa-Hori[1], S. Aizawa[2], N. Takahashi[1]**
[1]Division of Oral Ecology and Biochemistry, Department of Oral Biology and [2]Division of Pediatric Dentistry, Department of Lifelong Oral Health Sciences, Tohoku University Graduate School of Dentistry, Sendai, Japan

*Miyasawa-Hori H, Aizawa S, Takahashi N. Difference in the xylitol sensitivity of acid production among* Streptococcus mutans *strains and the biochemical mechanism. Oral Microbiol Immunol 2006: 21: 201–205.* © Blackwell Munksgaard, 2006.

Xylitol inhibits the glycolysis and growth of *Streptococcus mutans*, but to different degrees among strains. Thus, we studied the biochemical mechanism through which the inhibition varies, using *S. mutans* strains ATCC 31989, NCTN 10449, and NCIB 11723, which are highly sensitive, moderately sensitive, and resistant to xylitol, respectively, under strictly anaerobic conditions such as those found in deep layers of dental plaque. Xylitol (30 mM) decreased the rate of acid production from glucose (10 mM) in ATCC 31989, NCTC 10449, and NCIB 11723 by 86, 26, and 0%, respectively. The activities of the xylitol : phosphoenolpyruvate phosphotransferase system (PEP-PTS) relative to those of glucose : PEP-PTS were 120, 16, and 3%, respectively. In ATCC 31989 and NCTC 10449, intracellular accumulation of xylitol 5-phosphate and decreases of fructose 1,6-bisphosphate and glucose 6-phosphate were observed. Furthermore, in the presence of xylitol (30 mM), glucose : PEP-PTS activities decreased by 34, 17, and 0%, respectively. These findings indicated that the higher the xylitol : PEP-PTS activity was and the more effectively xylitol decreased glucose : PEP-PTS activity, the more sensitive the strain was to xylitol. These results suggest that the following inhibitory mechanisms are active in the xylitol-sensitive mutans streptococci: direct inhibition of glycolytic enzymes by xylitol 5-phosphate derived from xylitol : PEP-PTS and, possibly, indirect inhibition through competition for the phosphoryl donor, HPr-P, between glucose and xylitol : PEP-PTSs.

Key words: acid production; phosphoenolpyruvate-sugar phosphotransferase system; *Streptococcus mutans*; xylitol

Nobuhiro Takahashi, Division of Oral Ecology and Biochemistry, Department of Oral Biology, Tohoku University Graduate School of Dentistry, 4–1 Seiryo-machi, Aoba-ku, Sendai, 980–8575, Japan
Tel.: +81 22 7178294;
fax: +81 22 7178297;
e-mail: nobu-t@mail.tains.tohoku.ac.jp
Accepted for publication October 26, 2005

Xylitol is widely used as a noncariogenic sugar substitute because it is not fermented by oral bacteria (6). Xylitol has been reported to inhibit the growth of mutans streptococci in the presence of glucose, galactose, mannose, lactose, maltose, sucrose, sorbitol or mannitol as a carbon source *in vitro* (1, 5, 7, 8, 16, 24, 25), and the acid production from glucose by resting cells of *Streptococcus mutans* (7, 13, 25). Xylitol is also known to selectively inhibit the growth of *S. mutans* in mixed culture using a chemostat (3, 15).

The major route of sugar transport by microorganisms is via the phosphoenolpyruvate phosphotransferase system (PEP-PTS). Two sugar-nonspecific proteins, enzyme-I and histidine-containing phosphocarrier protein (HPr), and a sugar-specific protein, enzyme-II are required for PEP-PTSs. PEP phosphorylates enzyme-I to phospho-enzyme-I, which in turn transfers the phosphoryl group to HPr. In many cases, phospho-HPr (HPr-P) generated from phospho-enzyme-I, transfers the phosphoryl group directly to enzyme-II, which in turn phosphorylates incoming sugar (10, 14).

Bacterial cells are thought to incorporate xylitol as xylitol 5-phosphate through xylitol : PEP-PTS and the xylitol 5-phosphate inhibits the enzyme activity of sugar metabolism, resulting in the inhibition of both bacterial growth and acid production (18). In addition, the futile cycle, in which xylitol 5-phosphate is dephosphorylated to xylitol with waste of PEP potential, can also retard the growth of *S. mutans* (18).

However, some strains are xylitol sensitive whereas others are resistant (19), and the degree of inhibition varies among strains (25). Thus, we studied the biochemical mechanism of the variable inhibition, using three strains of *S. mutans* previously characterized as highly sensitive, moderately sensitive, and resistant to xylitol under strictly anaerobic conditions such as those found in deep layers of dental plaque.

## Material and methods

### Bacterial strains and growth conditions

We used the following strains of *S. mutans*: NCTC 10449, ATCC 31989, and NCIB 11723. *S. mutans* NCTC 10449 was a gift as a xylitol-sensitive strain from Prof. L. Trahan (Université Laval, Québec, Canada) (20). Each strain was inoculated into a complex medium containing 1.7% tryptone (Difco Laboratories, Detroit, MI), 0.3% yeast extract (Difco), 85 mM NaCl, and 11 mM glucose as described (25) under strictly anaerobic conditions in an anaerobic chamber ($N_2$, 80%; $H_2$, 10%; $CO_2$, 10%, NHC-type, Hirasawa Works, Tokyo, Japan) and incubated at 35°C overnight. Cell cultures were transferred into the same complex medium and precultured overnight at 35°C. The cell cultures were again transferred into the same complex medium (5% inoculum size) and grown at 35°C. The bacterial cells were harvested by centrifugation (7000 × *g* for 15 min at 4°C) at an early logarithmic phase of growth (optical density at 660 nm [$OD_{660}$] ≈ 0.3) under anaerobic conditions as described previously (17). Bacterial purity was regularly confirmed by culturing on blood agar plates.

### Acid production from glucose in the presence of xylitol

The following experiments were conducted in a different type of anaerobic chamber ($N_2$, 90%; $H_2$, 10%, NH-type, Hirasawa Works). Cells were washed twice with cold 2 mM potassium phosphate buffer (pH 7.0) containing 150 mM KCl and 5 mM $MgCl_2$, and suspended in the same buffer. The optical density of the cell suspension at 660 nm was adjusted to 3.5 (1.9 mg of cells [dry weight] per ml).

The cell suspensions were agitated with a magnetic stirrer at 35°C. The reaction was started by adding a mixture of 10 mM glucose and 0 or 30 mM xylitol to the cell suspensions. The rate of acid production by the cells was monitored at pH 7.0 using an automatic pH titrator (model AUT-211S, Toa Electronics Ltd, Kobe, Japan) with 50 mM KOH. The rate of acid production at 2 min after adding glucose or the glucose-xylitol mixture was calculated as μmol of protons per min per mg dry weight of cells.

Before and after the incubation for 10 min, cell suspensions (0.9 ml) were sampled and mixed immediately with 0.1 ml of 6 N perchloric acid. The mixtures were filtered (pore size 0.20 μm, polypropylene; ADVANTEC, Toyo Roshi Ltd, Tokyo, Japan) and cell-free filtrates were diluted with 0.2 N hydrochloric acid and stored at 4°C for the assay of acidic end products.

### Analysis of acidic end products

Amounts of acidic end products, lactic, acetic, formic and pyruvic acids were quantified using a carboxylic acid analyzer (model EYELA S-3000X; Tokyo Rikakikai Co., Ltd, Tokyo, Japan) in stored cell-free filtrates, as described previously (17).

### PEP-PTS activities for glucose, xylitol and fructose (glucose, xylitol and fructose : PEP-PTS activities)

The PEP-PTS activities were estimated by a modification of the method of Kornberg & Reeves (9) as described previously (13). Cells were harvested, washed twice as described above and stored at −20°C. After thawing, the cells were suspended in 2 mM potassium phosphate buffer (pH 7.0) containing 150 mM KCl and 5 mM $MgCl_2$ ($OD_{660}$ ≈ 5.0). Toluene was added at a final concentration of 1% to the cell suspension, and mixed vigorously for 1 min. After centrifugation (1200 × *g* for 3 min), the cells were suspended in the same buffer ($OD_{660}$ ≈ 50). The PEP-PTS activities for glucose, xylitol or fructose at pH 7.0 were estimated as a decrease of reduced nicotinamide adenine dinucleotide (NADH) in reaction mixtures containing 0.1 mM NADH, 53 μg of cells (dry weight)/ml, 1 mM phosphoenolpyruvate, 11 U/ml lactate dehydrogenase (EC 1.1.1.27, rabbit muscle; Roche Diagnostics, Indianapolis, IN) and 100 mM potassium phosphate buffer (pH 7.0) at 35°C. The reaction was started by adding 5, 10, 30, 60 or 120 mM glucose, xylitol or fructose. The decrease of NADH was monitored using a dual wavelength spectrophotometer (model 557; Hitachi Ltd, Tokyo, Japan) at 340 nm.

### Inhibition of glucose : PEP-PTS activity in the presence of xylitol

Glucose : PEP-PTS activity in the presence of xylitol was also determined. Toluene-treated cells as described above were suspended in a reaction mixture containing 1 mM NADP, 53 μg of cells [dry weight]/ml, 1 mM phosphoenolpyruvate, 3.5 U/ml glucose 6-phosphate dehydrogenase (EC 1.1.1.49, yeast; Roche Diagnostics) and 100 mM potassium phosphate buffer (pH 7.0) at 35°C. The reaction was started by adding 10 mM glucose and 0, 10, 30, 60 or 120 mM xylitol to the cell suspensions. The increase of NADPH was monitored spectrophotometrically at 340 nm.

### Assays of glycolytic intermediates and xylitol 5-phosphate

Cell suspensions were reacted with 10 mM glucose containing 0 or 30 mM xylitol as described above for the experiment of acid production. After the incubation for 2 min, the cells were collected by passing the reaction mixture through a membrane filter (pore size 0.45 μm, polyethersulfone; Acrodisc, Pall Gelman Laboratory, Ann Arbor, MI). Glycolytic intermediates and xylitol 5-phosphate in the cells were immediately extracted in 0.6 N perchloric acid, and neutralized with 5 M $K_2CO_3$ in air. The neutralized extracts were stored at 4°C for subsequent assays of the glycolytic intermediates and xylitol 5-phosphate, and at −20°C for 3-phosphoglycerate assays.

The glycolytic intermediates in the cell extracts were enzymatically determined at 35°C by a modification of the enzymatic method of Minakami et al. (12). Xylitol 5-phosphate was estimated as described previously (13). The assay mixture for xylitol 5-phosphate contained 1.1 mM NAD, 5 mM $MgCl_2$, 0.1 mM EDTA, and the extracts in 50 mM Tris-HCl buffer (pH 8.5) at 35°C. The reaction was started by the addition of 4.2 U/ml polyol dehydrogenase (EC 1.1.1.14, sorbitol dehydrogenase, sheep liver; Roche Diagnostics) and 50 U/ml alkaline phosphatase (EC 3.1.3.1, calf intestine; Roche Diagnostics). The increase of NADH was monitored spectrophotometrically at 340 nm.

### Statistical methods

Differences in rates of acid production, rates of glucose : PEP-PTS activities with xylitol and in profiles of glycolytic intermediates were analyzed by the Mann–Whitney *U*-test. Differences in amounts of

*Table 1.* Relative rate of acid production and the formation of acidic end products from 10 mM glucose (G) and 10 mM glucose plus 30 mM xylitol (G +X).

| *S. mutans* strain | Substrate | Relative rate of acid production | Acidic end products | | |
|---|---|---|---|---|---|
| | | | Lactate | Acetate | Formate |
| ATCC 31989 | G | 100 [a] | 1.44 ± 0.28[b] | 0.34 ± 0.09 | 0.34 ± 0.06 |
| | G +X | 14 ± 1# | 0.07 ± 0.01* | 0.25 ± 0.04 | 0.27 ± 0.04 |
| NCTC 10449 | G | 100 | 1.07 ± 0.07 | 0.92 ± 0.04 | 0.90 ± 0.05 |
| | G +X | 74 ± 9# | 0.42 ± 0.03 | 1.00 ± 0.07 | 1.11 ± 0.13 |
| NCIB 11723 | G | 100 | 1.72 ± 0.21 | 0.67 ± 0.08 | 0.75 ± 0.10 |
| | G +X | 102 ± 6 | 1.62 ± 0.22 | 0.69 ± 0.09 | 0.78 ± 0.12 |

[a] Relative rate of acid production (mean ± standard deviation, %) obtained from six independent experiments. Significant difference between relative rates of acid production in the presence and absence of xylitol: #$P < 0.01$.
[b]Amounts of acidic end products (mean ± standard deviation, μmol/mg cells) obtained from three independent experiments. Significant difference between amounts of acidic end products in the presence and absence of xylitol: *$P < 0.05$.

acidic end products were analyzed by the Dunn test.

## Results

### Inhibitory effect of xylitol on acid production

Xylitol significantly inhibited the acid production from glucose of *S. mutans* ATCC 31989 and NCTC 10449. In the presence of 30 mM xylitol, the acid production rates of ATCC 31989 and NCTC 10449 were decreased by 86 ± 1% ($P < 0.01$) and 26 ± 9% ($P < 0.01$), respectively, whereas that of NCIB 11723 was not inhibited (Table 1).

The total amounts of acidic end products generated by ATCC 31989 and NCTC 10449 cells decreased in the presence of xylitol. The reduction of lactic acid was remarkable and it was significant in ATCC 31989 ($P < 0.05$), resulting in an end product shift to formate-acetate-dominant (Table 1). Xylitol had no effect on NCIB11723.

### Glucose, xylitol and fructose : PEP-PTS activities

All *S. mutans* strains had PEP-PTS activities for glucose, xylitol, and fructose (Fig. 1). In ATCC 31989, fructose : PEP-PTS activity at 5–120 mM fructose and xylitol : PEP-PTS activity at 30–120 mM xylitol were higher than glucose : PEP-PTS activity. In particular, xylitol : PEP-PTS activity at 30 mM xylitol was 120 ± 14% of glucose : PEP-PTS activity at 10 mM glucose. In NCTC 10449, both fructose and xylitol : PEP-PTS activities were lower than glucose : PEP-PTS activity. Xylitol : PEP-PTS activity at 30 mM xylitol was 16 ± 6% of glucose : PEP-PTS activity at 10 mM glucose. Both fructose and xylitol : PEP-PTS activities were low in NCIB 11723, and xylitol : PEP-PTS at 30 mM xylitol activity was only 3 ± 1% of glucose : PEP-PTS activity at 10 mM glucose.

### Decrease in glucose : PEP-PTS activity in the presence of xylitol

In the presence of added xylitol, glucose : PEP-PTS activities of ATCC 31989 and NCTC 10449 were decreased (Fig. 2). The presence of 30 mM xylitol decreased glucose : PEP-PTS activity to 67 ± 6 and 83 ± 5%, respectively. As the xylitol concentration increased, the decrease became larger and statistically significant over 60 mM xylitol. However, little inhibition was observed in NCIB 11723.

### Effect of xylitol on the profile of glycolytic intermediates during glucose metabolism

When metabolizing glucose only, all of the *S. mutans* strains had large amounts of fructose 1,6-bisphosphate, but the profiles of glycolytic intermediates downstream of

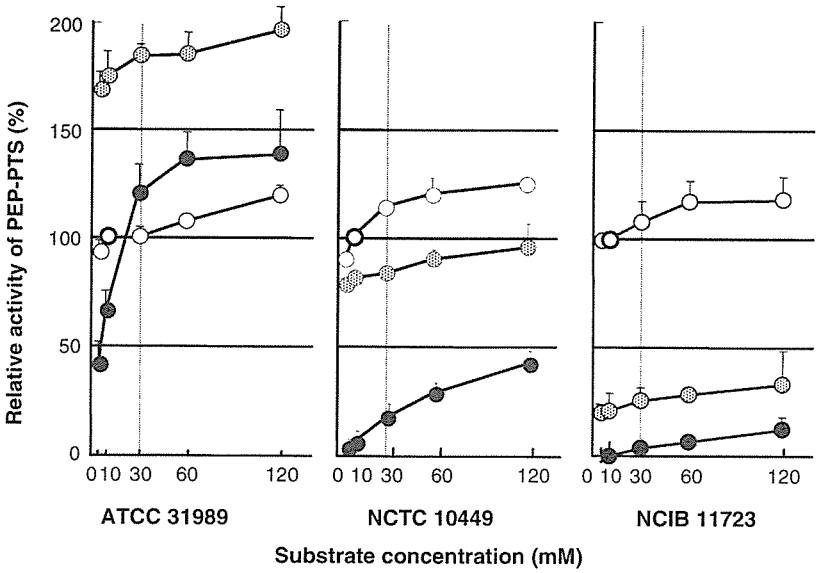


*Fig. 1.* PEP-PTS activities for glucose (○), xylitol (●) and fructose (◍) of *Streptococcus mutans* ATCC 31989, NCTC 10449, and NCIB 11723. Vertical bars indicate standard deviations from three independent experiments. PEP-PTS activity for 10 mM glucose was regarded as 100%.

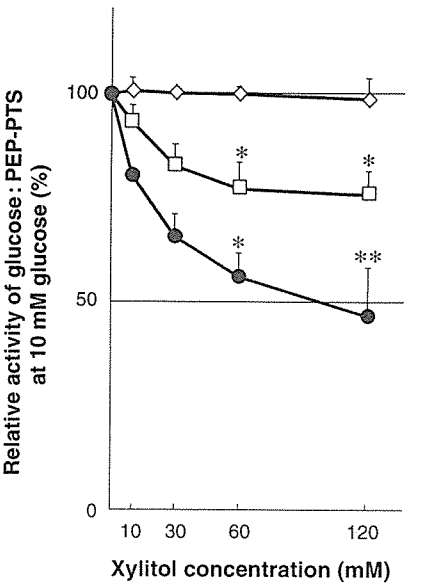


*Fig. 2.* PEP-PTS activities for 10 mM glucose of *Streptococcus mutans* in the presence of xylitol. ATCC 31989 (●), NCTC 10449 (□) and NCIB 11723 (◇). Significant difference between the PEP-PTS activities in the presence and absence of xylitol: *$P < 0.05$, **$P < 0.01$. Vertical bars indicate standard deviations from three independent experiments.

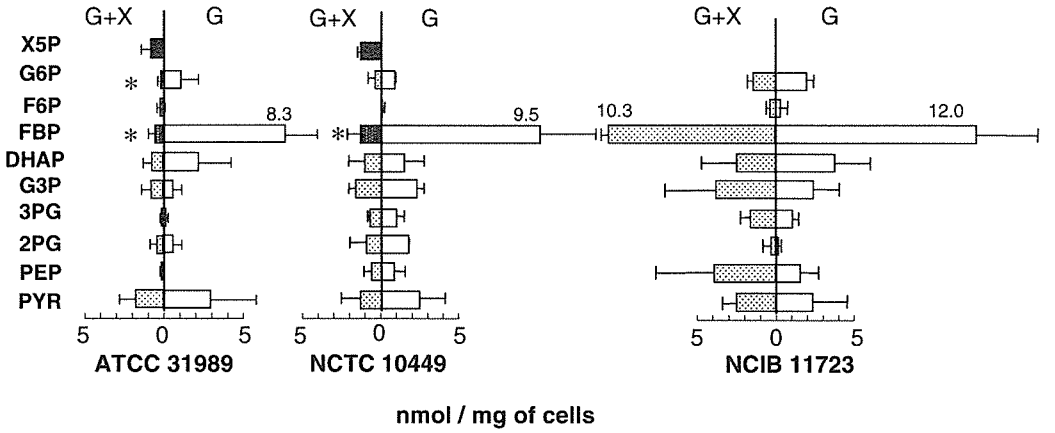


*Fig. 3.* Glycolytic intermediates and xylitol 5-phosphate of *S. mutans* ATCC 31989, NCTC 10449, and NCIB 11723 at 2 min after adding glucose (10 mM) or a mixture of glucose (10 mM) and xylitol (30 mM). Glycolytic intermediates (G, □) in the absence of xylitol. Glycolytic intermediate (G +X, ▨) and xylitol 5-phosphate (X5P, ■) in the presence of xylitol. G6P, glucose 6-phosphate; F6P, fructose 6-phosphate; FBP, fructose 1,6-bisphosphate; DHAP, dihydroxyacetone phosphate; G3P, glyceraldehyde 3-phosphate; 3PG, 3-phosphoglycerate; 2PG, 2-phosphoglycerate; PEP, phosphoenolpyruvate; PYR, pyruvate. Significant difference between intermediate levels in the presence and absence of xylitol: $*P = 0.05$. Horizontal bars indicate standard deviations from four independent experiments.

dihydroxyacetone phosphate were slightly different among strains (Fig. 3).

When glucose was being metabolized by the ATCC 31989 and NCTC 10449 strains in the presence of xylitol, xylitol 5-phosphate accumulated and the amounts of glycolytic intermediates decreased, particularly those of fructose 1,6-bisphosphate ($P = 0.05$) in ATCC 31989 and NCTC 10449 and glucose 6-phosphate (G6P) ($P = 0.05$) in ATCC 31989. However, such inhibition was not evident in NCIB 11723.

## Discussion

As previously reported (13, 25), xylitol inhibited the acid production of *S. mutans* strains and decreased the lactate production in strains ATCC 31989 and NCTC 10449 (Table 1), but the degree of these inhibitions varied between strains. On the other hand, in strain NCIB 11723, xylitol did not inhibit acid production or shift the end product profile.

Trahan (18) proposed an inhibitory mechanism of xylitol in which *S. mutans* transports xylitol as xylitol 5-phosphate through the activity of xylitol : PEP-PTS and, consequently, the xylitol 5-phosphate inhibits phosphoglucose isomerase and phosphofructokinase, the glycolytic enzymes for G6P conversion to fructose 1,6-bisphosphate, resulting in a decrease in intracellular levels of fructose 1,6-bisphosphate and the entire glycolytic rate. Miyasawa et al. (13) and Maehara et al. (11) then confirmed this notion, and found the decrease in lactate production was due to the decrease in fructose 1,6-bisphosphate, an absolute activator of streptococcal lactate dehydrogenase. The present study found that higher xylitol : PEP-PTS activity indicated more inhibition of acid production by xylitol (Table 1 and Fig. 1). This observation supports the notion that xylitol 5-phosphate produced by xylitol : PEP-PTS activity is responsible for glycolytic inhibition and suggests that *S. mutans* strains with higher xylitol : PEP-PTS activity are more sensitive to xylitol inhibition. It has been proposed that xylitol is transported via a constitutive fructose : PEP-PES and that xylitol : PEP-PTS activity appears as part of the constitutive fructose : PEP-PTS activity (18, 19, 22). We found here that high fructose : PEP-PTS activities in *S. mutans* were accompanied by high xylitol : PEP-PTS activities (Fig. 1), supporting this notion. Furthermore, it is reported that the *fxpC* gene of the constitutive fructose : PEP-PTS was located in the genomes of xylitol-sensitive streptococci and the *fxpC*-defective mutant was resistant to xylitol (2), although no information is available about *fxpC* gene in the strains used in our study.

Analyses of metabolic intermediates revealed that the xylitol-sensitive strains ATCC 31989 and NCTC 10449 accumulated xylitol 5-phosphate and decreased fructose 1,6-bisphosphate in the presence of xylitol (Fig. 3). These results support the notion that xylitol inhibits the glycolytic enzymes required for G6P conversion to fructose 1,6-bisphosphate. Despite the powerful inhibitory effect of xylitol (Table 1) and high xylitol : PEP-PTS activity (Fig. 1), the accumulation of xylitol 5-phosphate in ATCC 31989 seemed to be smaller than that in NCTC 10449. It is suggested that the glycolytic enzymes of ATCC 31989 are more sensitive to xylitol and a small amount of xylitol 5-phosphate is enough to inhibit the entire glycolytic metabolism.

Not only fructose 1,6-bisphosphate but also G6P significantly decreased in a highly xylitol-sensitive strain ATCC 31989 (Fig. 3), indicating that xylitol itself can inhibit the glucose uptake system (e.g. glucose : PEP-PTS) and result in a decrease in intracellular G6P. This was confirmed by the observation that the presence of xylitol decreased the glucose : PEP-PTS activity in xylitol-sensitive strains, ATCC 31989 and NCTC 10449 (Fig. 2). This could be due to competition for the phosphoryl donor, HPr-P, between the glucose and the xylitol : PEP-PTSs. In the ATCC 31989 strain, with high xylitol : PEP-PTS activity and powerful xylitol inhibition of glucose : PEP-PTS activity, HPr-P could phosphorylate xylitol to xylitol 5-phosphate efficiently and result in a direct inhibition by xylitol 5-phosphate on glycolytic enzymes and an indirect inhibition on glucose phosphorylation by HPr-P.

NCIB 11723 isolated from human dental plaque by Carlsson (4) has natural xylitol resistance like other xylitol-resistant strains isolated from xylitol consumers (21, 23). It has been suggested that the xylitol resistance is due to the absence of a constitutive fructose : PEP-PTS by which xylitol is also incorporated, thus preventing xylitol-resistant strains from incorporating xylitol (19, 21). In the present study, NCIB 11723 had little xylitol : PEP-PTS

activity (Fig. 1) and did not accumulate xylitol 5-phosphate (Fig. 3) in the presence of a low concentration of xylitol, supporting this notion. As the xylitol concentration increased, however, xylitol : PEP-PTS activities of NCIB 11723 appeared (Fig. 1). In the presence of 120 mM xylitol, the xylitol : PEP-PTS activity compared with that of glucose : PEP-PTS reached 12 ± 4%. However, 120 mM xylitol did not inhibit glucose : PEP-PTS activity (Fig. 2) and negligibly inhibited acid production from glucose (data not shown). These findings indicate that xylitol has less affinity for HPr-P than glucose in NCIB 11723. Thus, the strain cannot incorporate xylitol as xylitol 5-phosphate in the presence of both xylitol and glucose.

In conclusion, xylitol sensitivity varies among *S. mutans* strains: the higher the xylitol : PEP-PTS activity, and the more effectively xylitol decreases glucose : PEP-PTS activity, the more sensitive the strain is to xylitol. Xylitol has two inhibitory mechanisms:

- direct inhibition of glycolytic enzymes by xylitol 5-phosphate derived from xylitol : PEP-PTS;
- possibly, indirect inhibition of sugar uptake through competition for the phosphoryl donor, HPr-P, between the glucose and the xylitol : PEP-PTS.

## Acknowledgments

This study was supported in part by a research fellowship (no. 16·3025 to HH) and Grants-in-Aid for Scientific Research (B) (no. 16390601 to NT) from the Japan Society for the Promotion of Science.

## References

1. Assev S, Wåler SM, Rölla G. Further studies on the growth inhibition of some oral bacteria by xylitol. Acta Pathol Microbiol Immunol Scand [B] 1983: **91**: 261–265.
2. Benchabane H, Lortie LA, Buckley ND, Trahan L, Frenette M. Inactivation of the *Streptococcus mutans fxpC* gene confers resistance to xylitol, a caries-preventive natural carbohydrate sweetener. J Dent Res 2002: **81**: 380–386.
3. Bradshaw DJ, Marsh PD. Effect of sugar alcohols on the composition and metabolism of a mixed culture of oral bacteria grown in a chemostat. Caries Res 1994: **28**: 251–256.
4. Carlsson J. Presence of various types of non-haemolytic streptococci in dental plaque and in other sites of the oral cavity in man. Odontol Revy 1967: **18**: 55–74.
5. Gauthier L, Vadeboncoeur C, Mayrand D. Loss of sensitivity to xylitol by *Streptococcus mutans* LG-1. Caries Res 1984: **18**: 289–295.
6. Gehring F, Mäkinen KK, Larmas M, Scheinin A. Turku sugar studies. IV. An intermediate report on the differentiation of polysaccharide-forming streptococci (*S. mutans*). Acta Odontol Scand 1974: **32**: 435–444.
7. Kakuta H, Iwami Y, Mayanagi H, Takahashi N. Xylitol inhibition of acid production and growth of mutans streptococci in the presence of various dietary sugars under strictly anaerobic conditions. Caries Res 2003: **37**: 404–409.
8. Kenney EB, Ash MM. Oxidation reduction potential of developing plaque, periodontal pockets and gingival sulci. J Periodontol 1969: **40**: 630–633.
9. Kornberg HL, Reeves RE. Inducible phosphoenolpyruvate-dependent hexose phosphotransferase activities in *Escherichia coli*. Biochem J 1972: **128**: 1339–1344.
10. Lengeler JW, Jahreis K, Wehmeier UF. Enzymes II of the phosphoenolpyruvate-dependent phosphotransferase systems: their structure and function in carbohydrate transport. Biochim Biophys Acta 1994: **1188**: 1–28.
11. Maehara H, Iwami Y, Mayanagi H, Takahashi N. Synergistic inhibition by combination of fluoride and xylitol on glycolysis by mutans streptococci and its biochemical mechanism. Caries Res 2005: **39**: 521–528.
12. Minakami S, Suzuki C, Saito T, Yoshikawa H. Studies on erythrocyte glycolysis. I. Determination of the glycolytic intermediates in human erythrocytes. J Biochem 1965: **58**: 543–550.
13. Miyasawa H, Iwami Y, Mayanagi H, Takahashi N. Xylitol inhibition of anaerobic acid production by *Streptococcus mutans* at various pH levels. Oral Microbiol Immunol 2003: **18**: 215–219.
14. Postma PW, Lengeler JW, Jacobson GR. Phosphoenolpyruvate: carbohydrate phosphotransferase systems of bacteria. Microbiol Rev 1993: **57**: 543–594.
15. Rogers AH, Pilowsky KA, Zilm PS, Gully NJ. Effects of pulsing with xylitol on mixed continuous cultures of oral streptococci. Aust Dent J 1991: **36**: 231–235.
16. Rölla G, Oppermann RV, Waaler SM, Assev S. Effect of aqueous solutions of sorbitol-xylitol on plaque metabolism and on growth of *Streptococcus mutans*. Scand J Dent Res 1981: **89**: 247–250.
17. Takahashi N, Abbe K, Takahashi-Abbe S, Yamada T. Oxygen sensitivity of sugar metabolism and interconversion of pyruvate formate-lyase in intact cells of *Streptococcus mutans* and *Streptococcus sanguis*. Infect Immun 1987: **55**: 652–656.
18. Trahan L. Xylitol: a review of its action on mutans streptococci and dental plaque – its clinical significance. Int Dent J 1995: **45**: 77–92.
19. Trahan L, Bareil M, Gauthier L, Vadeboncoeur C. Transport and phosphorylation of xylitol by a fructose phosphotransferase system in *Streptococcus mutans*. Caries Res 1985: **19**: 53–63.
20. Trahan L, Bourgeau G, Breton R. Emergence of multiple xylitol-resistant (fructose PTS-) mutants from human isolates of mutans streptococci during growth on dietary sugars in the presence of xylitol. J Dent Res 1996: **75**: 1892–1900.
21. Trahan L, Mouton C. Selection for *Streptococcus mutans* with an altered xylitol transport capacity in chronic xylitol consumers. J Dent Res 1987: **66**: 982–988.
22. Trahan L, Neron S, Bareil M. Intracellular xylitol-phosphate hydrolysis and efflux of xylitol in *Streptococcus sobrinus*. Oral Microbiol Immunol 1991: **6**: 41–50.
23. Trahan L, Soderling E, Drean MF, Chevrier MC, Isokangas P. Effect of xylitol consumption on the plaque-saliva distribution of mutans streptococci and the occurrence and long-term survival of xylitol-resistant strains. J Dent Res 1992: **71**: 1785–1791.
24. Vadeboncoeur C, St Martin S, Brochu D, Hamilton IR. Effect of growth rate and pH on intracellular levels and activities of the components of the phosphoenolpyruvate: sugar phosphotransferase system in *Streptococcus mutans* Ingbritt. Infect Immun 1991: **59**: 900–906.
25. Vadeboncoeur C, Trahan L, Mouton C, Mayrand D. Effect of xylitol on the growth and glycolysis of acidogenic oral bacteria. J Dent Res 1983: **62**: 882–884.

Histochem Cell Biol (2006) 126: 371–380
DOI 10.1007/s00418-006-0171-8

ORIGINAL PAPER

**Hidetoshi Mitani · Ichiro Takahashi · Kazuyuki Onodera
Jin-Wan Bae · Takuichi Sato · Nobuhiro Takahashi
Yasuyuki Sasano · Kaoru Igarashi · Hideo Mitani**

# Comparison of age-dependent expression of aggrecan and ADAMTSs in mandibular condylar cartilage, tibial growth plate, and articular cartilage in rats

Accepted: 2 March 2006 / Published online: 1 April 2006


**Abstract** A disintegrin and metalloproteinase with thrombospondin motif (adamalysin–thrombospondins, ADAMTS) degrades aggrecan, one of the major extracellular matrix (ECM) components in cartilage. Mandibular condylar cartilage differs from primary cartilage, such as articular and growth plate cartilage, in its metabolism of ECM, proliferation, and differentiation. Mandibular condylar cartilage acts as both articular and growth plate cartilage in the growing period, while it remains as articular cartilage after growth. We hypothesized that functional and ECM differences between condylar and primary cartilages give rise to differences in gene expression patterns and levels of aggrecan and ADAMTS-1, -4, and -5 during growth and aging. We employed in situ hybridization and semiquantitative RT-PCR to identify mRNA expression for these molecules in condylar cartilage and primary cartilages during growth and aging. All of the ADAMTSs presented characteristic, age-dependent expression patterns and levels among the cartilages tested in this study. ADAMTS-5 mainly contributed to ECM metabolism in growth plate and condylar cartilage during growth. ADAMTS-1 and ADAMTS-4 may be involved in ECM turn over in articular cartilage. The results of the present study reveal that ECM metabolism and expression of related proteolytic enzymes in primary and secondary cartilages may be differentially regulated during growth and aging.

**Keywords** ADAMTS · Aggrecan · Mandibular condylar cartilage · Articular cartilage · Growth plate · Growth · Aging

H. Mitani · I. Takahashi (✉) · K. Onodera · J. W. Bae
K. Igarashi · H. Mitani
Division of Orthodontics and Dentofacial Orthopedics,
Tohoku University Graduate School of Dentistry,
4-1 Seiryo-machi, Aoba-ku, Sendai, 980-8575, Japan
E-mail: takahasi@mail.tains.tohoku.ac.jp
Tel.: +81-22-7178374
Fax: +81-22-7178378

T. Sato · N. Takahashi
Division of Oral Ecology and Biochemistry, Tohoku University Graduate School of Dentistry, 4-1 Seiryo-machi, Aoba-ku, Sendai, 980-8575, Japan

Y. Sasano
Division of Craniofacial Development and Regeneration, Tohoku University Graduate School of Dentistry, 4-1 Seiryo-machi, Aoba-ku, Sendai, 980-8575, Japan

K. Igarashi
Division of Oral Dysfunction Science, Tohoku University Graduate School of Dentistry, 4-1 Seiryo-machi, Aoba-ku, Sendai, 980-8575, Japan

## Introduction

Aggrecanase is a member of the metalloproteinase family which degrades a major cartilaginous extracellular matrix (ECM) component, aggrecan (Abbaszade et al. 1999; Arner et al. 1999; Tortorella et al. 1999; Caterson et al. 2000; Tang 2001; Arner 2002). Three members of the adamalysin–thrombospondins (ADAMTSs), ADAMTS-1, -4 (aggrecanase-1), and -5 (aggrecanase-2), are capable of cleaving an aggrecan molecule (Abbaszade et al. 1999; Tortorella et al. 1999; Kuno et al. 2000) at its specific sites, in a different manner from matrix metalloproteinases (MMPs), another large family of ECM degrading enzymes. Together with MMPs, ADAMTSs play a role in cartilage ECM metabolism during the development of cartilage and progression of joint diseases (Lohmander et al. 1993; Fosang et al. 1996; Lark et al. 1997; Caterson et al. 2000; Sandy and Verscharen 2001). Most studies have focused on the activity of aggrecanases, especially their production and activation under disease conditions, such as inflammatory responses and joint diseases, whereas their physiological expression patterns have not been determined during growth and aging.

Synovial joints are classified into two types, primary joints, such as the knee, and secondary joints, such as the temporomandibular joint (TMJ) (Ten Cate 1994). In

primary joints, primary articular and growth plate cartilages function separately for articulation and growth, respectively, whereas mandibular condylar cartilage performs both of these functions during growing period. ECM components and cellular organization of mandibular condylar cartilage, as a secondary cartilage, are different from those of primary cartilages as demonstrated previously (Silbermann et al. 1987; Luder et al. 1988; Mizoguchi et al. 1992). While mandibular condylar cartilage has been shown to have five distinct layers, primary cartilages, including growth plate and articular cartilage, is composed of four layers during the growth period (Luder et al. 1988; Mizoguchi et al. 1992). Primary cartilage cells express both type II collagen and aggrecan, cartilage-specific ECM components; however, cells in the upper two layers of mandibular condylar cartilage do not express either of these molecules (Mizoguchi et al. 1992; Takahashi et al. 1996; Shibata et al. 2001). Proliferating cells in growth plate and articular cartilage are well-differentiated chondrocytes, but those in mandibular condylar cartilage are not (Mizoguchi et al. 1992). Thus, cell proliferation and matrix synthesis in mandibular condylar cartilage are regulated differently from those of primary cartilages. In addition, during the growth, development, and maturation of the synovial joints, growth plate cartilage disappears by the end of the growth period. Similar to articular cartilage, which remains in the epiphysis of long bones, mandibular condylar cartilage becomes articular cartilage by losing hypertrophic chondrocytes after growth. Therefore, it can be considered that ECM metabolism in primary and mandibular condylar cartilage is differently regulated.

In this study, we examined the hypothesis that functional and ECM differences between condylar and primary cartilage give rise to differences in gene expression patterns and levels of ADAMTS-1, -4, and -5 during growth and aging. To test this hypothesis we used semiquantitative reverse transcriptase polymerase chain reaction (RT-PCR) and in situ hybridization (ISH) using a newly identified rat ADAMTS-5 mRNA and subcloned aggrecan, ADAMTS-1 and ADAMTS-4.

## Materials and methods

### Experimental animals and tissue preparation

Male Wistar rats 4, 8, 16, and 32 weeks old were used in this study. Five animals for each age group were perfused via the ascending aorta with 4% paraformaldehyde and 0.5% glutaraldehyde in phosphate-buffed saline (PBS), pH 7.4, under pentobarbital anesthesia as described previously (Sasano et al. 1996). Procedures for tissue preparation were basically identical to our previous report (Bae et al. 2003). After the animals were perfused, TMJs and knee joints were dissected, further fixed in the same fixatives, and decalcified in 10% ethylene diamine tetra-acetic acid (EDTA). They were dehydrated, embedded in paraffin, and 8-μm-thick sagittal sections were cut for ISH analysis under RNase-free conditions and hematoxylin and eosin (H&E) staining. Animal experiments were conducted under the approval of the Animal Care and Use Committee of Tohoku University, Japan.

### Cloning aggrecan and ADAMTSs and generating cRNA probes

Reverse transcriptase polymerase chain reaction-based cloning was employed to obtain partial or full clones of each molecule. Based on the homology between mouse and human ADAMTS-5 cDNA sequences, degenerate amplimers were designed as shown in Table 1. For other molecules, amplimers were designed based on the cDNA sequences of rats shown in Table 1 and in our previous study (Nakamura et al. 2005). PCR conditions used in the present study are also summarized in Table 1. The cDNA fragments obtained were subcloned into pCRII-TOPO vector (Invitrogen, Carlsbad, CA, USA), according to the manufacturer's instructions. Nucleic acid sequences of ADAMTS-5 were analyzed by the dye-terminating method using ALF express II sequencer (Amersham Pharmacia Biotech, Buckinghamshire, UK) and the other fragments were analyzed by Takara (Osaka, Japan) to confirm the nucleic acid sequences. To create Dig-labeled riboprobes for sense and antisense fragments, the plasmids were linearized and transcribed by using Sp6 or T7 RNA polymerases (Stratagene, La Jolla, CA, USA) into cRNA as indicated in Table 1.

### In situ hybridization

The protocol for ISH has been described previously (Ohtani et al. 1992; Sasano et al. 1996; Zhu et al. 2001). Sections were deparaffinized, rehydrated, and immersed in 0.2 N HCl for 20 min at room temperature, then incubated with 20 μg/ml proteinase K (Roche Diagnostics, Indianapolis, IN, USA) at 37°C for 30 min. After sections were dehydrated in ethanol, they were hybridized with approximately 400 ng/ml riboprobes at 45°C for 16 h. Sections were incubated with 20 μg/ml RNase A (Sigma, St Louis, MO, USA) in 1× SSC (saline–sodium citrate buffer) during stringent wash in 2× SSC and 1× SSC at 45°C. After sections were incubated with anti-Dig alkaline phosphatase-conjugated antibody (Roche Diagnostics) at 4°C overnight in a moisture chamber, signals were visualized and nuclear counterstaining was performed using methyl green. Sections were mounted and observed under light microscopy.

### Semiquantitative RT-PCR

Gene expression of aggrecan and ADAMTS-1, -4, and -5 were semiquantified by RT-PCR in three types of cartilage. Bilateral mandibular condylar, growth plate, and articular cartilages were dissected from 4-week-old and adult male Wistar rats killed by ether anesthesia.

**Table 1** Conditions for cloning, creating riboprobes and semi-quantitative RT-PCR

| Gene name and accession no. | Nucleic acid sequences of amplimers | PCR annealing temperature(°C) | Product length (bp) | Cycle number for semi-quantitative RT-PCR | Restriction enzymes for | | RNA polymerase |
|---|---|---|---|---|---|---|---|
| Aggrecan | Upstream | GTTAGTGGAGGGCGTGAC | 55 | 634 | 32 cycles | Anti-sense | *Eco*RV | Sp6 |
| NM_022190 | Downstream | CTTGGCTGTTTCTGCTGTT | | | | Sense | *Bam*HI | T7 |
| ADAMTS-1 | Upstream-1 | GTTGGGAAAGGAAAGCAGA | 68 | 1,123 | – | Anti-sense | *Eco*RV | Sp6 |
| NM_024400 | Downstream-1 | AGGGTTGTGGCAGGAAATA | | | | Sense | *Bam*HI | T7 |
| | Upstream-2 | GGCGGAGGACGAAGAGT | 62 | 445 | 48 cycles | – | – | – |
| | Downstream-2 | GGAAGCGAGGAGTAGCAAC | | | | | | |
| ADAMTS-4 | Upstream | CTACAACCACCGAACCGAC | 60 | 602 | 48 cycles | Anti-sense | *Spe*I | T7 |
| XM_237904 | Downstream | TGCCAGCCACCAGAACTT | | | | Sense | *Eco*RV | Sp6 |
| ADAMTS-5 | Upstream-1 | ATGCKNCTYGRNTGGGC | 60 | 1,395 | – | NA | NA | NA |
| AF142099 | Downstream-1 | ACCGTCATCCAGAAATTC | | | | NA | NA | NA |
| NM_011782 | Upstream-2 | GATCTCTAGAATCATTCATG TGACACCCTG | 60 | 1,685 | – | Anti-sense | *Spe*I | Sp6 |
| | Downstream-2 | GATCTCTAGAAACCACAGGCT AACATTTC | | | | Sense | *Xho*I | T7 |
| | Upstream-3 | GGCTGTGGTGTGCTGTG | 58 | 758 | 48 cycles | – | – | – |
| | Downstream-3 | CTGGTCTTTGGCTTTGAAC | | | | | | |
| GAPDH | Upstream | TGTTTGTGATG GTGTGAA | 56 | 485 | 30 cycles | – | – | – |
| MN_017008 | Downstream | ATGGGAGTTGCTGTTGAG | | | | | | |

Mandibular condyles and tibial epiphysis were removed from mandibular bone and tibia, respectively. Cartilaginous tissues in the articular surfaces of mandibular condyle and tibia were removed carefully under dissection microscope in ice-cold PBS by using fine scalpels. After articular cartilage was obtained, bone tissue in secondary ossification center and cartilaginous tissue fragments of remained articular cartilage were carefully removed, then growth plates were separated from tibial epiphysis of 4-week-old rats. The specimens were frozen in liquid nitrogen and homogenized in lysis buffer to isolate total RNA using the RNeasy Lipid Tissue Mini Kit (Qiagen, Hilden, Germany) following the manufacturer's instructions. Standardized 200 ng amounts of total RNA were reverse transcribed before PCR amplification. PCR conditions and number of reaction cycles were empirically determined by drawing amplification curves at each annealing temperature for each molecule (Table 1). Optical density from each amplified product separated on 2% agarose gel was digitized and measured using NIH imaging software (National Institutes of Health, Bethesda, MD, USA), and relative gene expression levels were semi-quantified against glyceraldehyde-3-phosphate dehydrogenase. Expression levels were statistically analyzed by Scheffe's test.

## Results

### Cloning rat ADAMTS-5

The deduced amino acid sequence of rat ADAMTS-5 is shown in Fig. 1, aligned with human and mouse ADAMTS-5. The coding sequence of rat ADAMTS-5 mRNA consists of 2,787 bp (GenBank Accession No. AY382879), which generates 928 amino acid residues. Rat ADAMTS-5 mRNA had 93.6 and 84.9% homology with that of mice and humans, respectively. The amino acid sequence of rat ADAMTS-5 showed 96.2 and 90.3% homology to that of mice and humans, respectively. Rat ADAMTS-5 protein lacked two amino acid residues in the metalloproteinase domain at $Asp^{326}$ and $Thr^{327}$ when compared to mouse ADAMTS-5. Pre- and pro-domains were less conserved in rats when compared to mice or humans. The domain structure of ADAMTS-5 in rats was identical to that in other species with a metalloproteinase domain including a catalytic domain, two thrombospondine-1 motifs, and a disintegrin-like motif.

### Histological observation (Figs. 2, 3)

During the growth period, mandibular condylar cartilage consisted of five cell layers: a fibrous layer with fibroblasts embedded in the fibrous connective tissue, a proliferative cell layer with undifferentiated and proliferating polygonal cells, a transitional cell layer with flattened cells without cytosolic lipid droplets, a mature cell layer, and a hypertrophic cell layer (Fig. 2a, b). Tibial

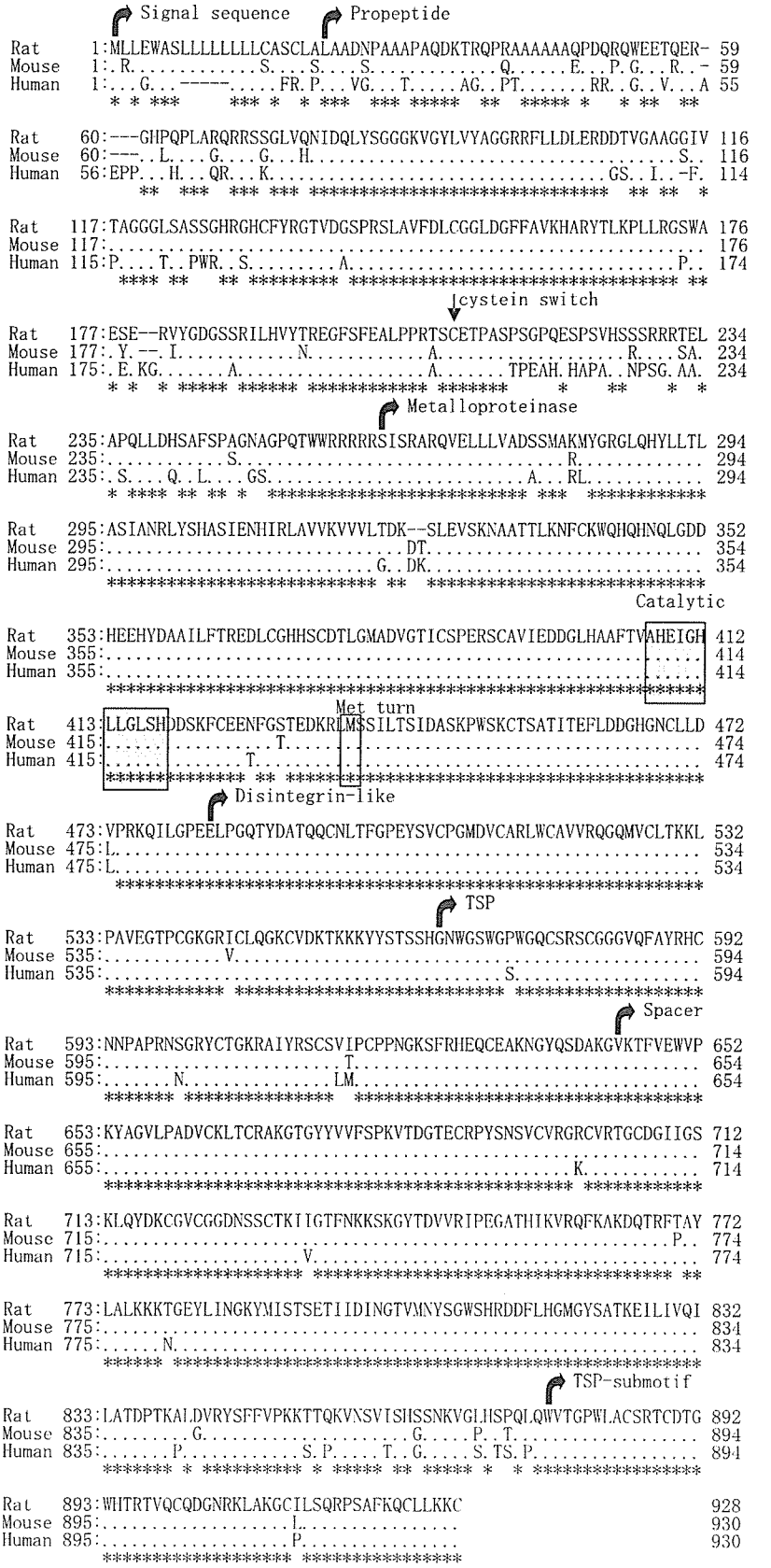


**Fig. 1** The amino acid sequence deduced from the ADAMTS-5 cDNA is shown aligned with those of human and mouse ADAMTS-5. Residues matching the consensus sequence of the three proteins are *dotted* in the human and mouse sequences. The conserved zinc-binding motif and "Met turn" are *boxed*. *TSP* thrombospondin motif

epiphyseal growth plate cartilage and articular cartilage consisted of four layers: a resting cell layer with chondrocytes, which was the smallest in size of all the layers; a proliferative cell layer with flattened, proliferating cells; a mature cell layer containing ovoid-shaped well-differentiated chondrocytes with lipid drops; and a hypertrophic

cell layer consisting of enlarged cells with disorganized cytosolic structures during the growth period (Fig. 3a, b). Mandibular condylar cartilage showed characteristics of growth plate cartilage with a hypertrophic cell layer at the lower border involved in endochondral bone formation during growth. In contrast, mandibular condylar cartilage at 16 and 32 weeks of age mainly consisted of three layers: a resting cell layer, a proliferating cell layer, and a mature cell layer (Fig. 2c, d), and closely resembled articular cartilage lacking the hypertrophic cell layer seen in younger animals (Fig. 3c). The uppermost layer of aged mandibular condylar cartilage was a fibrous layer with elongated fibroblasts embedded in fibrous connective tissue, the second layer was a proliferating cell layer consisting of small proliferating cells, and the lower layer was a mature cell layer with well-differentiated chondrocytes, including some hypertrophic cells (Fig. 2c, d). Tibial articular cartilage consisted of three layers at 32 weeks of age (Fig. 3c).

Gene expression patterns (Figs. 4, 5, 6)

*Age 4 and 8 weeks (Figs. 4, 5)*

At 4 and 8 weeks of age, positive hybridization signals for aggrecan were observed in mature and hypertrophic chondrocytes in condylar, articular, and the growth plate cartilage (Figs. 4a, e, 5a, e). While condylar cartilage did not show positive signals for aggrecan in the upper three layers (Fig. 4a, e), a positive signal was observed in the resting and proliferating cell layers in both articular and growth plate cartilage (Fig. 5a, e). ADAMTS-1

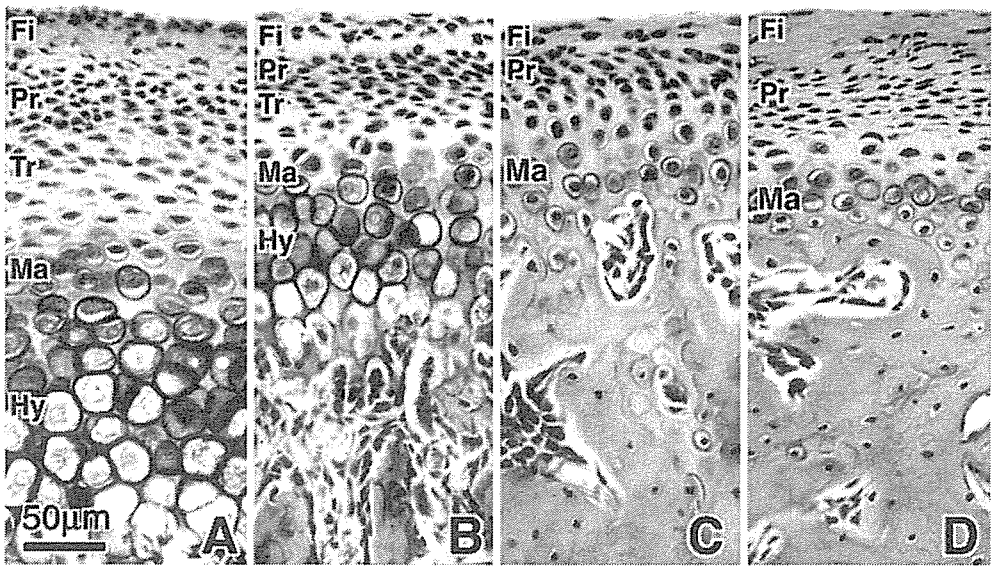


**Fig. 2** Sagittal sections of mandibular condylar cartilage stained with H&E from 4-week-old (**a**), 8-week-old (**b**), 16-week-old (**c**), and 32-week-old (**d**) rats. *Fi* fibrous layer; *Pr* proliferative cell layer; *Tr* transitional cell layer; *Ma* mature cell layer; *Hy* hypertrophic cell layer. *Scale bar* 50 μm; original magnification: ×40

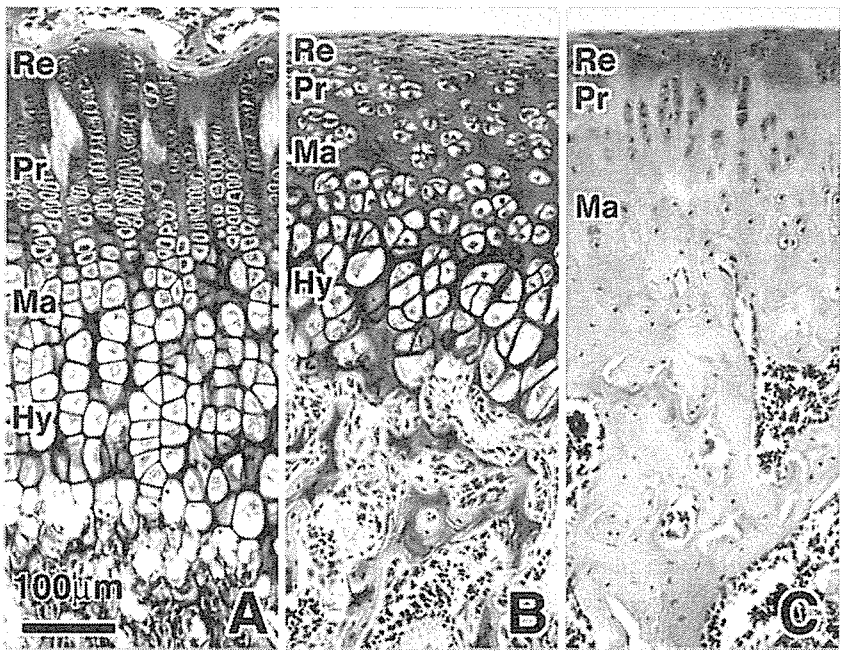


**Fig. 3** Sagittal sections of growth plate and articular cartilage stained with H&E. Growth plate cartilage from 4-week-old rats (**a**) and articular cartilage from 4-week-old (**b**), and 32-week-old (**c**) rats. *Re* resting cell layer; *Pr* proliferative cell layer; *Ma* mature cell layer; *Hy* hypertrophic cell layer. *Scale bar* 100 μm; original magnification: ×20

expression was observed in all of the cell layers in the three types of cartilage during growth (Figs. 4b, f, 5b, f). In condylar cartilage, mature chondrocytes showed the strongest hybridization signals to ADAMTS-1 compared to the other layers at ages 4 and 8 weeks (Fig. 4b, f). The cells in the transitional cell layer and below were positive for ADAMTS-4 in condylar cartilage, with the strongest expression in hypertrophic chondrocytes (Fig. 4c, g). Cells in all four layers showed positive signals for ADAMTS-4 in growing articular cartilage at 4 weeks (Fig. 5g), while cells in the proliferating cell layer were negative in growth plate cartilage (Fig. 5c). ADAMTS-5 showed positive hybridization signals localized in mature and hypertrophic chondrocytes in both condylar (Fig. 4d, h) and growth plate cartilage (Fig. 5d), while it was observed in all cell layers in articular cartilage at 4 weeks of age (Fig. 5h). During the growth period, the expression domain of aggrecan covered that of ADAMTS-5, while other ADAMTSs had a greater expression domain than that of aggrecan, especially ADAMTS-1, which was expressed ubiquitously in all types of cartilage during the growth period. In addition, all types of ADAMTSs were expressed in all four layers of articular cartilage during growth.

*Age 16 and 32 weeks (Fig. 6)*

After growth was completed and the hypertrophic cell layer disappeared, positive hybridization signals for aggrecan were localized in mature chondrocytes of condylar and articular cartilage (Fig. 6a, e, i). With aging, aggrecan expression was maintained in the well-differentiated chondrocytes in the mature cell layers. However, the strength of the hybridization signal decreased with age. The hybridization signal for ADAMTS-1 in the fibrous layer, which was positive at 8 weeks (Fig. 4b, f), was negative at 16 and 32 weeks (Fig. 6b, f). Consequently, the area negative for ADAMTS-1 in condylar cartilage expanded from the fibrous layer to the proliferating cell layer by 32 weeks (Fig. 6b, f). The hybridization signal for ADAMTS-1 remained in all of the cell layers in articular cartilage at 32 weeks of age (Fig. 6j). ADAMTS-4 was

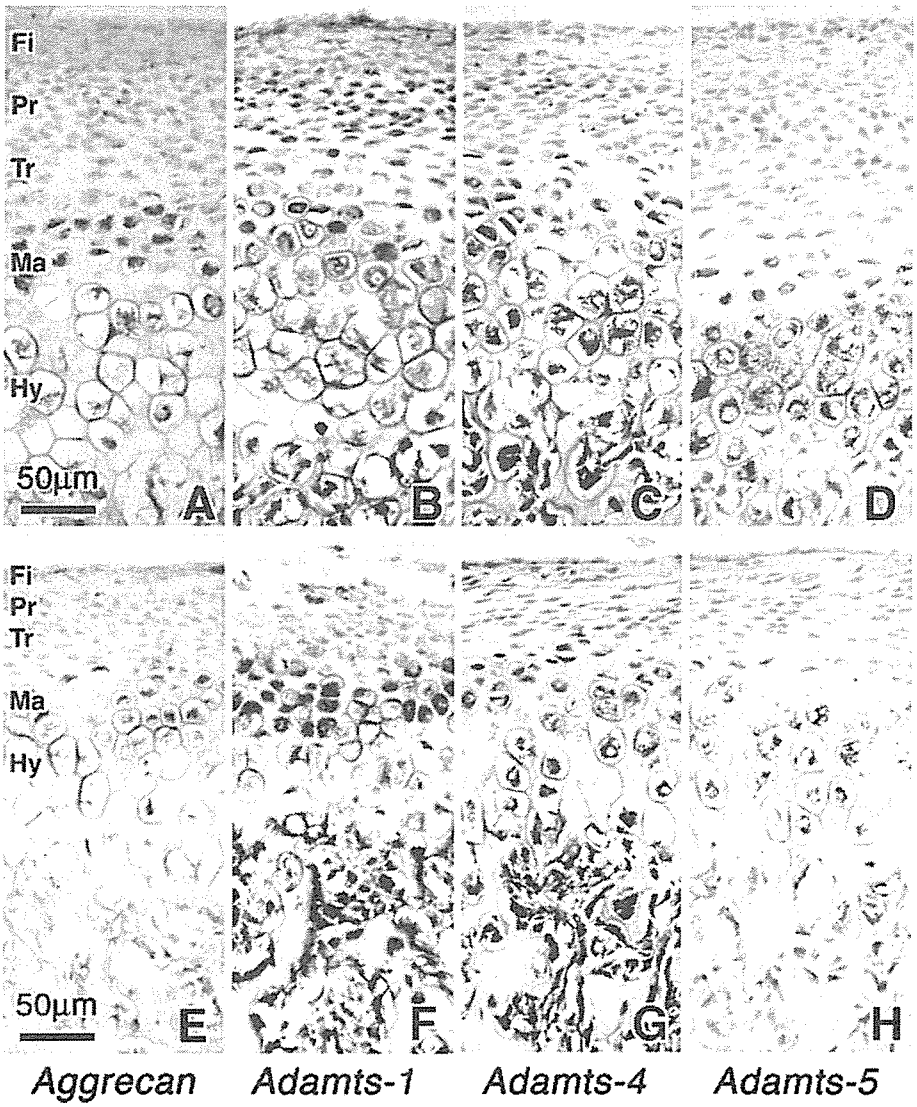


**Fig. 4** In situ hybridization analysis for aggrecan (**a**, **e**), ADAMTS-1 (**b**, **f**), ADAMTS-4 (**c**, **g**), and ADAMTS-5 (**d**, **h**) of sagittal sections of mandibular condylar cartilage from 4-week-old (**a**–**d**) and 8-week-old (**e**–**h**) rats. *Fi* fibrous layer; *Pr* proliferative cell layer; *Tr* transitional cell layer; *Ma* mature cell layer; *Hy* hypertrophic cell layer. Brown-purple staining in the cytosol is a positive hybridization signal. *Scale bar* 50 μm; original magnification: ×40

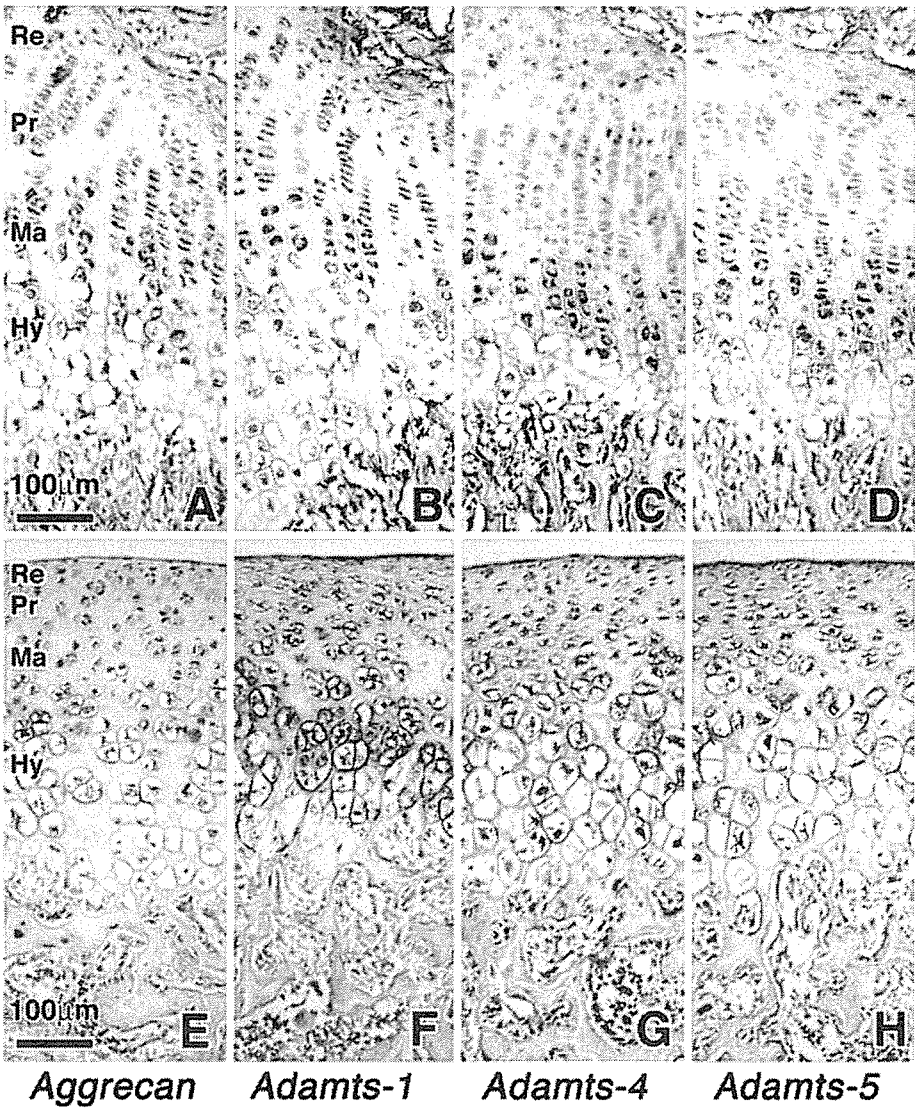


**Fig. 5** In situ hybridization analysis for aggrecan (**a**, **e**), ADAMTS-1 (**b**, **f**), ADAMTS-4 (**c**, **g**), and ADAMTS-5 (**d**, **h**) of sagittal sections of growth plate (**a–d**) and articular cartilage (**e–h**). *Re* resting cell layer; *Pr* proliferative cell layer; *Ma* mature cell layer; *Hy* hypertrophic cell layer. Brown-purple staining in the cytosol is a positive hybridization signal. *Scale bar* 100 μm; original magnification: ×20

localized in mature chondrocytes at 16 weeks of age (Fig. 6c) and remained so at 32 weeks of age in condylar cartilage (Fig. 6g). It was only localized in mature chondrocytes in articular cartilage (Fig. 6k). ADAMTS-5 was expressed in the lower part of the mature cell layers in condylar cartilage at 16 and 32 weeks (Fig. 6d, h), while it was not expressed in aged articular cartilage (Figs. 6l, 7).

Gene expression levels

The expression level of all ADAMTSs examined was maintained during aging in mandibular condylar cartilage, whereas that of ADAMTS-4 and -5 decreased in articular cartilage during aging (Fig. 7a, b). ADAMTS-4 expression in growth plate cartilage was significantly lower than that in articular cartilage at the same age (Fig. 7a, b). Gene expression levels of aggrecan and ADAMTS-1 were similar in all types of cartilage and at all ages examined, while slightly, but not significantly, less expression of ADAMTS-1 was observed in aged mandibular condylar cartilage (Fig. 7a, b).

## Discussion

ADAMTS-5 is also known as aggrecanase-2, which cleaves aggrecan, one of the cartilage-specific macromolecules (Doege et al. 1991). While all three ADAMTS genes examined have been identified in mice, cattle, and humans, this is the first time that ADAMTS-5 has been identified in rats. Rat ADAMTS-5 conserved all of the domains seen in mice and humans (Abbaszade et al. 1999). Since rat ADAMTS-5 lacks two amino acid residues in the metalloproteinase domain and the catalytic domain is conserved completely when compared to humans and mice, aggrecanase activity of ADAMTS-5 may differ in rats from other species.

The age-dependent changes in aggrecan expression in condylar cartilage were similar to those of type II collagen demonstrated previously (Ohashi et al. 1997; Bae et al. 2003); expression and localization of type II collagen becomes restricted to mature cell layers as aging progresses. In addition, the expression pattern of versican is

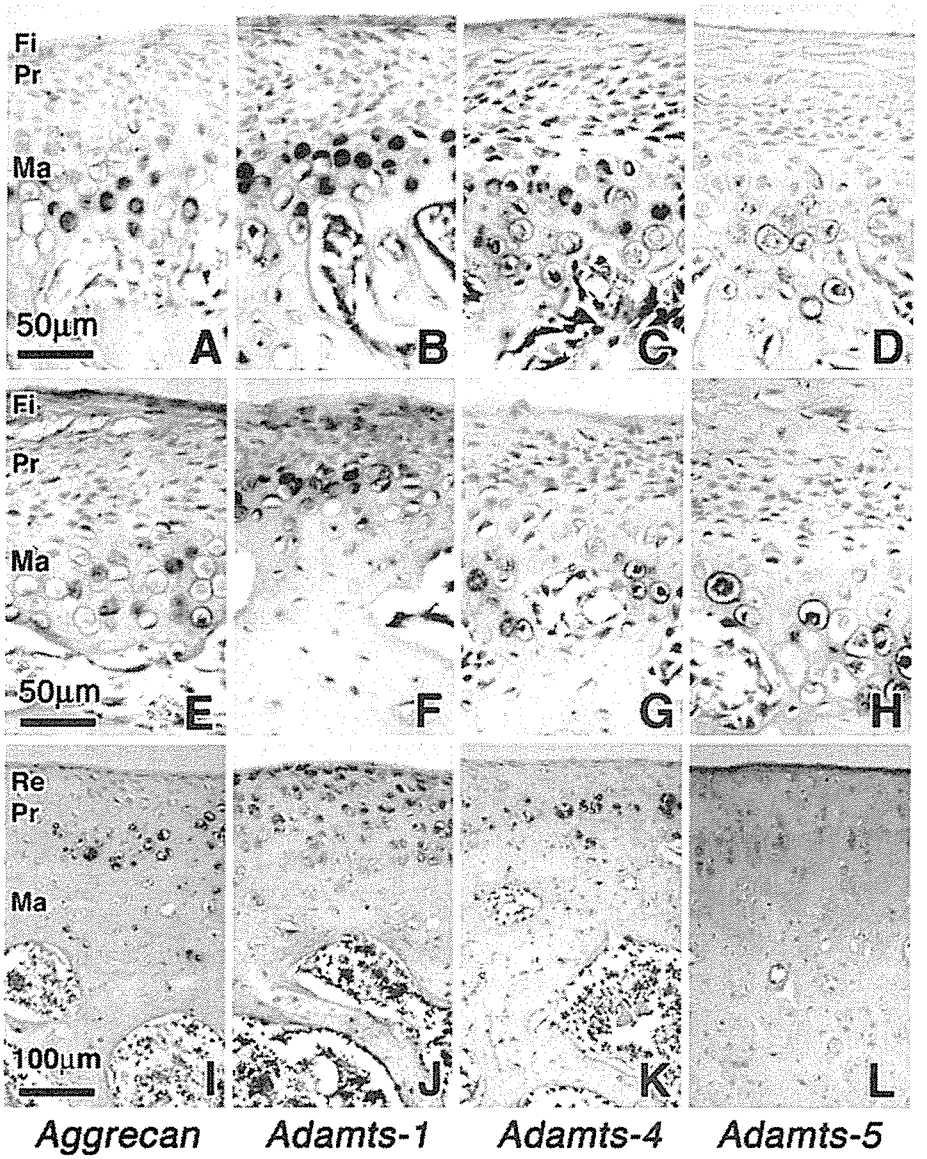


**Fig. 6** In situ hybridization analysis for aggrecan (**a**, **e**, **i**), ADAMTS-1 (**b**, **f**, **j**), ADAMTS-4 (**c**, **g**, **k**), and ADAMTS-5 (**d**, **h**, **l**) of sagittal sections of mandibular condylar cartilage from 16-week-old (**a–d**) and 32-week-old (**e–h**) rats and articular cartilage from 32-week-old (**i–l**) rats. *Re* resting cell layer; *Fi* fibrous layer; *Pr* proliferative cell layer; *Ma* mature cell layer. Brown-purple staining in the cytosol is a positive hybridization signal. *Scale bar* in **a–h** 50 μm and **i–l** 100 μm; original magnification: ×40 (**a–h**) and ×20 (**i–l**)

regulated differently in condylar and primary cartilage during growth (Shibata et al. 2001). While versican is co-expressed with aggrecan in primary cartilage, its expression is restricted to the fibrous layer of condylar cartilage, while aggrecan is expressed in the mature and hypertrophic cell layer during embryonic growth. Several researchers have investigated the substrate specificity of the three ADAMTSs: ADAMTS-1 cleaves aggrecan and versican (Kuno et al. 2000; Sandy and Verscharen 2001); ADAMTS-4 cleaves aggrecan, brevican, and versican (Matthews et al. 2000; Nakamura et al. 2000; Tortorella et al. 2000; Sandy and Verscharen 2001; Sztrolovics et al. 2002); and ADAMTS-5 cleaves aggrecan (Abbaszade et al. 1999; Arner 2002). Since ADAMTS-1 is the only ADAMTS among those examined in the present study that is expressed in the fibrous layer of condylar cartilage, it may contribute to versican metabolism in this layer. Thus, specific expression patterns of each ADAMTS may reflect the expression of their specific substrates during endochondral ossification.

Tibial growth plate and mandibular condyle are sites of endochondral bone formation. Chondrocytes in the growth plate and condylar cartilage deposit cartilaginous ECM components such as aggrecan and type II collagen to provide a template that is subsequently replaced by bone tissue. Cell volume increases as chondrocytes differentiate during this process (Luder et al. 1988). Besides the expression of ADAMTSs, chondrocytes produce several types of MMP during growth (Bae et al. 2003; Gepstein et al. 2003). Therefore, once deposited, ECM components such as type II collagen and aggrecan are degraded by aggrecanases in combination with MMPs. ADAMTS-5, mainly expressed in mature and hypertrophic chondrocytes in both condylar and growth plate cartilage, may provide space for expanding chondrocytes during terminal differentiation. In addition, recent studies have demonstrated that targeted

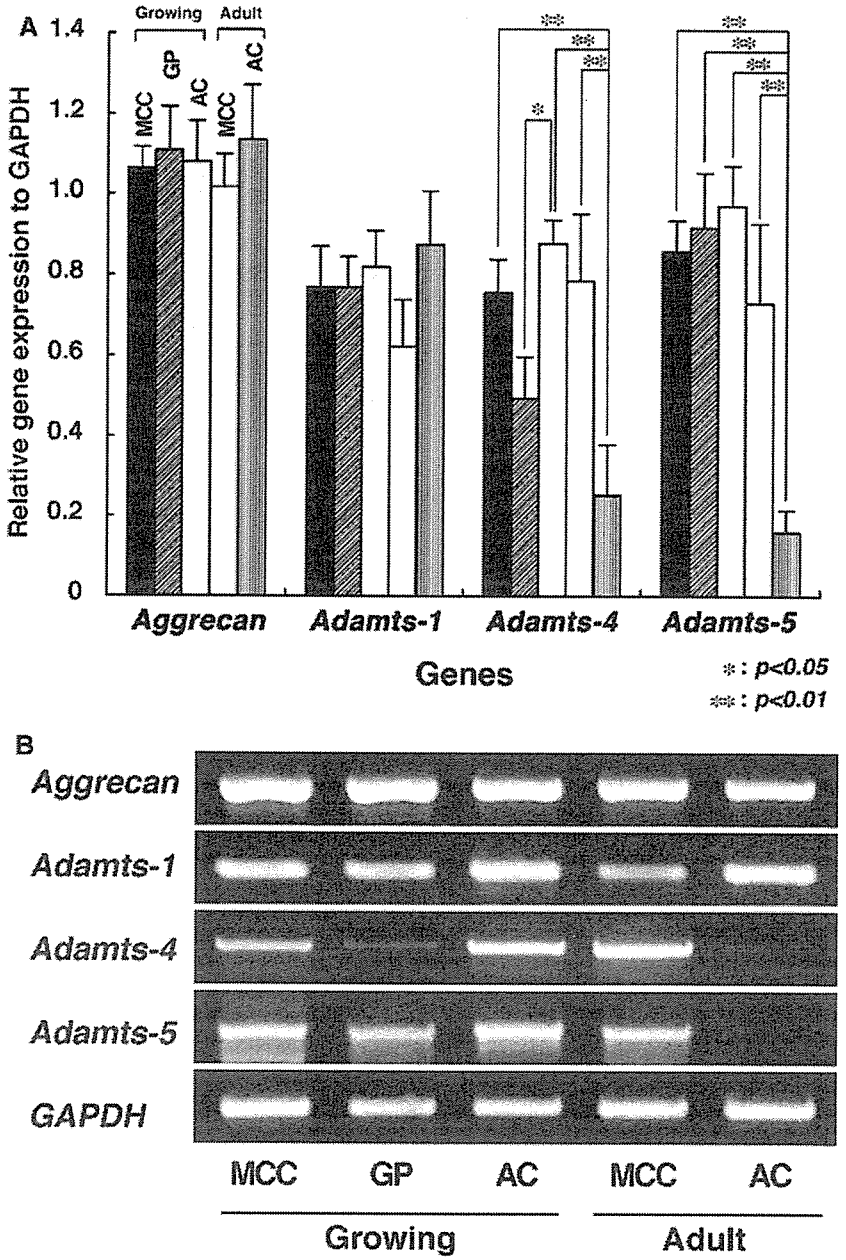


**Fig. 7** Graph indicating the results of semiquantitative RT-PCR (**a**) and representative images of agarose gel electrophoresis (**b**) ($n=3$). *MCC* mandibular condylar cartilage (*closed bar* growing; *open bar* adult); *GP* growth plate cartilage (*oblique stripe bar*); and *AC* articular cartilage (*shaded bar* growing; *vertical stripe bar* adult). $*P<0.05$ and $**P<0.01$

disruption of active ADAMTS-5, but not ADAMTS-4, inhibits experimentally induced inflammatory degeneration of cartilage (Glasson et al. 2005; Stanton et al. 2005) in growing mice. Therefore, it may be that ADAMTS-5 is a major aggrecanolytic enzyme contributing not only to such pathological processes, but also to physiological degradation of ECM molecules during the growth period.

After growth, all ADAMTSs expressed in the mature chondrocytes of condylar cartilage may play a role in the physiological turnover of aggrecan in order to maintain cartilage tissue. However, ADAMTS-1 and ADAMTS-4, but not ADAMTS-5, could contribute to the physiological turnover of aggrecan in aged articular cartilage. Therefore, ECM remodeling in aged mandibular condylar cartilage could be regulated differently from that in articular cartilage.

In summary, ADAMTS-5 appears to contribute mainly to degradation of ECM molecules such as aggrecan in growth plate and condylar cartilage, depending upon its ECM composition and cellular organization during growth. In conclusion, the results of the present study reveal that ECM metabolism by ADAMTSs and expression of ADAMTSs in primary and secondary cartilage may be differentially regulated during growth and aging, depending upon the functional differences in different types of cartilage.

**Acknowledgments** We thank Dr. Manabu Kagayama, Professor Emeritus of the Graduate School of Dentistry, Tohoku University, Japan, for his instructions and valuable advice during this project. This research was supported by Grants-in-Aid (#11771308, #12557180, and #15390550) from the Japanese Ministry of Education, Culture, Sports, Science and Technology.

## References


Abbaszade I, Liu RQ, Yang F, Rosenfeld SA, Ross OH, Link JR, Ellis DM, Tortorella MD, Pratta MA, Hollis JM, Wynn R, Duke JL, George HJ, Hillman MC Jr, Murphy K, Wiswall BH, Copeland RA, Decicco CP, Bruckner R, Nagase H, Itoh Y, Newton RC, Magolda RL, Trzaskos JM, Burn TC et al (1999) Cloning and characterization of ADAMTS11, an aggrecanase from the ADAMTS family. J Biol Chem 274:23443–23450

Arner EC (2002) Aggrecanase-mediated cartilage degradation. Curr Opin Pharmacol 2:322–329

Arner EC, Pratta MA, Trzaskos JM, Decicco CP, Tortorella MD (1999) Generation and characterization of aggrecanase. A soluble, cartilage-derived aggrecan-degrading activity. J Biol Chem 274:6594–6601

Bae JW, Takahashi I, Sasano Y, Onodera K, Mitani H, Kagayama M, Mitani H (2003) Age-related changes in gene expression patterns of matrix metalloproteinases and their collagenous substrates in mandibular condylar cartilage in rats. J Anat 203:235–241

Caterson B, Flannery CR, Hughes CE, Little CB (2000) Mechanisms involved in cartilage proteoglycan catabolism. Matrix Biol 19:333–344

Doege KJ, Sasaki M, Kimura T, Yamada Y (1991) Complete coding sequence and deduced primary structure of the human cartilage large aggregating proteoglycan, aggrecan. Human-specific repeats, and additional alternatively spliced forms. J Biol Chem 266:894–902

Fosang AJ, Last K, Maciewicz RA (1996) Aggrecan is degraded by matrix metalloproteinases in human arthritis. Evidence that matrix metalloproteinase and aggrecanase activities can be independent. J Clin Invest 98:2292–2299

Gepstein A, Arbel G, Blumenfeld I, Peled M, Livne E (2003) Association of metalloproteinases, tissue inhibitors of matrix metalloproteinases, and proteoglycans with development, aging, and osteoarthritis processes in mouse temporomandibular joint. Histochem Cell Biol 120:23–32

Glasson SS, Askew R, Sheppard B, Carito B, Blanchet T, Ma HL, Flannery CR, Peluso D, Kanki K, Yang Z, Majumdar MK, Morris EA (2005) Deletion of active ADAMTS5 prevents cartilage degradation in a murine model of osteoarthritis. Nature 434:644–648

Kuno K, Okada Y, Kawashima H, Nakamura H, Miyasaka M, Ohno H, Matsushima K (2000) ADAMTS-1 cleaves a cartilage proteoglycan, aggrecan. FEBS Lett 478:241–245

Lark MW, Bayne EK, Flanagan J, Harper CF, Hoerrner LA, Hutchinson NI, Singer II, Donatelli SA, Weidner JR, Williams HR, Mumford RA, Lohmander LS (1997) Aggrecan degradation in human cartilage. Evidence for both matrix metalloproteinase and aggrecanase activity in normal, osteoarthritic, and rheumatoid joints. J Clin Invest 100:93–106

Lohmander LS, Neame PJ, Sandy JD (1993) The structure of aggrecan fragments in human synovial fluid. Evidence that aggrecanase mediates cartilage degradation in inflammatory joint disease, joint injury, and osteoarthritis. Arthritis Rheum 36:1214–1222

Luder HU, Leblond CP, von der Mark K (1988) Cellular stages in cartilage formation as revealed by morphometry, radioautography and type II collagen immunostaining of the mandibular condyle from weanling rats. Am J Anat 182:197–214

Matthews RT, Gary SC, Zerillo C, Pratta M, Solomon K, Arner EC, Hockfield S (2000) Brain-enriched hyaluronan binding (BEHAB)/brevican cleavage in a glioma cell line is mediated by a disintegrin and metalloproteinase with thrombospondin motifs (ADAMTS) family member. J Biol Chem 275:22695–22703

Mizoguchi I, Nakamura M, Takahashi I, Kagayama M, Mitani H (1992) A comparison of the immunohistochemical localization of type I and type II collagens in craniofacial cartilages of the rat. Acta Anat 144:59–64

Nakamura H, Fujii Y, Inoki I, Sugimoto K, Tanzawa K, Matsuki H, Miura R, Yamaguchi Y, Okada Y (2000) Brevican is degraded by matrix metalloproteinases and aggrecanase-1 (ADAMTS4) at different sites. J Biol Chem 275:38885–38890

Nakamura M, Sone S, Takahashi I, Mizoguchi I, Echigo S, Sasano Y (2005) Expression of versican and ADAMTS1, 4, and 5 during bone development in the rat mandible and hind limb. J Histochem Cytochem 53:1553–1562

Ohashi N, Ejiri S, Hanada K, Ozawa H (1997) Change in type I, II, and X collagen immunoreactivity of the mandibular condylar cartilage in a naturally aging rat model. J Bone Miner Metab 15:77–83

Ohtani H, Kuroiwa A, Obinata M, Ooshima A, Nagura H (1992) Identification of type I collagen-producing cells in human gastrointestinal carcinomas by non-radioactive in situ hybridization and immunoelectron microscopy. J Histochem Cytochem 40:1139–1146

Sandy JD, Verscharen C (2001). Analysis of aggrecan in human knee cartilage and synovial fluid indicates that aggrecanase (ADAMTS) activity is responsible for the catabolic turnover and loss of whole aggrecan whereas other protease activity is required for C-terminal processing in vivo. Biochem J 358:615–626

Sasano Y, Furusawa M, Ohtani H, Mizoguchi I, Takahashi I, Kagayama M (1996) Chondrocytes synthesize type I collagen and accumulate the protein in the matrix during development of rat tibial articular cartilage. Anat Embryol 194:247–252

Shibata S, Fukada K, Suzuki S, Ogawa T, Yamashita Y (2001) Histochemical localization of versican, aggrecan and hyaluronan in the developing condylar cartilage of the fetal rat mandible. J Anat 198:129–135

Silbermann M, Reddi AH, Hand AR, Leapman RD, von der Mark K, Franzen A (1987) Further characterization of the extracellular matrix in the mandibular condyle in neonatal mice. J Anat 151:169–188

Stanton H, Rogerson FM, East CJ, Golub SB, Lawlor KE, Meeker CT, Little CB, Last K, Farmer PJ, Campbell IK, Fourie AM, Fosang AJ (2005) ADAMTS5 is the major aggrecanase in mouse cartilage in vivo and in vitro. Nature 434:648–652

Sztrolovics R, Grover J, Cs-Szabo G, Shi SL, Zhang Y, Mort JS, Roughley PJ (2002) The characterization of versican and its message in human articular cartilage and intervertebral disc. J Orthop Res 20:257–266

Takahashi I, Mizoguchi I, Sasano Y, Saitoh S, Ishida M, Kagayama M, Mitnai H (1996) Age-related changes in the localization of glycosaminoglycans in condylar cartilage of the mandible in rats. Anat Embryol 194:489–500

Tang BL (2001) ADAMTS: a novel family of extracellular matrix proteases. Int J Biochem Cell Biol 33:33–44

Ten Cate AR (1994) Temporomandibular joint In: Ten Cate AR (ed) Oral histology: development, structure, and function, 4th edn. Mosby, St. Louis, pp 432–455

Tortorella MD, Burn TC, Pratta MA, Abbaszade I, Hollis JM, Liu R, Rosenfeld SA, Copeland RA, Decicco CP, Wynn R, Rockwell A, Yang F, Duke JL, Solomon K, George H, Bruckner R, Nagase H, Itoh Y, Ellis DM, Ross H, Wiswall BH, Murphy K, Hillman MC Jr, Hollis GF, Newton RC, Magolda RL, Trzaskos JM, Arner EC (1999) Purification and cloning of aggrecanase-1: a member of the ADAMTS family of proteins. Science 284:1664–1666

Tortorella M, Pratta M, Liu RQ, Abbaszade I, Ross H, Burn T, Arner E (2000) The thrombospondin motif of aggrecanase-1 (ADAMTS-4) is critical for aggrecan substrate recognition and cleavage. J Biol Chem 275:25791–25797

Zhu JX, Sasano Y, Takahashi I, Mizoguchi I, Kagayama M (2001) Temporal and spatial gene expression of major bone extracellular matrix molecules during embryonic mandibular osteogenesis in rats. Histochem J 33:25–35

*Renya Sato*
*Takuichi Sato*
*Ichiro Takahashi*
*Junji Sugawara*
*Nobuhiro Takahashi*

# Profiling of bacterial flora in crevices around titanium orthodontic anchor plates

**Authors' affiliations:**
*Renya Sato, Ichiro Takahashi, Junji Sugawara,* Division of Orthodontics and Dentofacial Orthopedics, Tohoku University Graduate School of Dentistry, Sendai, Japan
*Takuichi Sato, Nobuhiro Takahashi,* Division of Oral Ecology and Biochemistry, Tohoku University Graduate School of Dentistry, Sendai, Japan

**Correspondence to:**
*Takuichi Sato, DDS, PhD*
Division of Oral Ecology and Biochemistry
Tohoku University Graduate School of Dentistry
Sendai 980-8575
Japan
Tel.: +81 22 717 8295
Fax: +81 22 717 8297
e-mail: tak@mail.tains.tohoku.ac.jp

**Date:**
Accepted 15 February 2006

**To cite this article:**
Sato R, Sato T, Takahashi I, Sugawara J, Takahashi N. Profiling of bacterial flora in crevices around titanium orthodontic anchor plates.
*Clin. Oral Impl. Res.* **18**, 2007; 21–26
doi: 10.1111/j.1600-0501.2006.01294.x



**Key words:** bacteria, bone screws, orthodontic appliances, polymerase chain reaction, 16S ribosomal RNA

**Abstract**

**Objectives:** The aims of this study were to characterize the microflora in crevices around titanium orthodontic anchor plates using anaerobic culture and molecular biological techniques for bacterial identification, and to compare the microbial composition between crevices around anchor plates and gingival crevices.

**Material and methods:** Samples from crevices around titanium anchor plates and healthy gingival crevices of 17 subjects (aged 20–29) were cultured anaerobically, and isolated bacteria were identified by 16S rRNA sequencing.

**Results:** The average logarithm colony-forming units/ml were 6.84, 7.51 and 8.88 in healthy anchor plate crevices, inflamed anchor plate crevices and healthy gingival crevices, respectively, indicating that the bacterial density of anchor plate crevices was lower than that of healthy gingival crevices. Of 184 strains isolated from healthy anchor plate crevices of seven subjects, 108 (59%) were anaerobic bacteria, while 73 (40%) were facultative bacteria. Predominant isolates were Gram-negative rods, such as *Campylobacter* (12%), *Fusobacterium* (10%) and *Selenomonas* (10%), and Gram-positive facultative bacteria, such as *Actinomyces* (17%) and *Streptococcus* (8.2%). Of 133 strains isolated from inflamed anchor plate crevices of three subjects, 110 (83%) were anaerobic bacteria, while predominant isolates were Gram-negative rods, such as *Prevotella* (47%), *Fusobacterium* (33%) and *Campylobacter* (16%). On the other hand, of 146 strains isolated from healthy gingival crevices of seven subjects, 98 (67%) were facultative bacteria, while 45 (31%) were anaerobic bacteria. Predominant isolates were Gram-positive facultative bacteria, such as *Actinomyces* (37%) and *Streptococcus* (20%).

**Conclusions:** These results suggest that the environment in crevices around titanium orthodontic anchor plates is anaerobic and supportive of anaerobic growth of bacteria, which may trigger inflammation in the tissue around the plates.

Microbial flora at the interface between histocompatible artificial material and mucosal epithelium is one of the most important factors for the prognosis of dental implants (Mombelli et al. 1987; Rosenberg et al. 1991; van Winkelhoff et al. 2000). It has been reported that Gram-negative obligate anaerobes predominantly comprised the bacterial flora in peri-implantitis pockets as well as periodontal pockets (Mombelli et al. 1987), whereas Gram-positive facultative anaerobes are predominant in healthy peri-implant crevices of successful implants (Mombelli & Mericske-Stern 1990). Another study verified that the microflora around clinically stable implants was similar to that of healthy gingival sulcus, and that microflora in peri-

implantitis were similar to that in periodontal pockets (Haanaes 1990).

Currently, titanium mini-plates as well as titanium mini-screws and dental implants have been applied as an absolute anchorage for tooth movement in orthodontic therapy, such as the skeletal anchorage system (SAS) (Umemori et al. 1999; Sugawara et al. 2002, 2004). However, approximately 10% of SAS anchor plate cases have developed acute inflammatory responses during orthodontic treatment (Nagasaka et al. 1999), and in the worst cases, the anchor plates were removed due to inflammation. Similarly, microbial flora in crevices around the anchor plates is one of the critical factors for the stability of implanted anchor plates and subsequent orthodontic treatment. However, there is no information on the nature of the microflora in anchor plate crevices under healthy and inflammatory conditions.

Therefore, the aims of this study were to characterize the microflora in crevices around titanium anchor plates using anaerobic culture for isolation of obligate anaerobes and molecular biological techniques for bacterial identification, as well as comparing the microbial composition between healthy and inflamed crevices.

## Material and methods

### Subjects

Seven periodontally healthy subjects with SAS using titanium mini-plates (age, 20–29 years; mean, 23.7 years) and three subjects with symptoms of swelling, pus discharge and spontaneous pain around the implanted titanium anchor plates at sampling (age, 23–25 years; mean, 24 years) were randomly selected for this study. In addition, seven periodontally healthy subjects (without SAS; age, 23–26 years; mean, 24.7 years) were also included in this study (Table 1).

Subjects were medically healthy by history, and received no antibiotics for 3 weeks preceding the sampling. Furthermore, they had neither anamnesis of pregnancy, genetic disease nor smoking habits.

### Clinical oral examination

All subjects were examined for plaque accumulation by plaque index (Silness & Löe 1964), gingival inflammation by gingival index (Löe & Silness 1963) and probing depth using a periodontal pocket probe. Subjects were considered periodontally healthy based on clinical evaluation of plaque index $\leq 1$ (Silness & Löe 1964) and gingival index $\leq 1$ (Löe & Silness 1963), and no signs of acute inflammation; and there were no instances of probeable gingival sulcus depth greater than 3 mm or alveolar bone loss.

### Sampling procedure

Sampling sites were isolated by cotton rolls, and supramucosal or supragingival plaque was carefully removed with a sterilized spoon excavator and pledget. Fluids from each transmucosal pocket (of seven healthy anchor plate crevices and three inflamed anchor plate crevices) around SAS implanted on zygomatic buttress, of which arms were placed beside the upper first molars (Fig. 1) were sampled with a micropipet, as described previously (Uematsu & Hoshino 1992). In addition, from seven periodontally healthy subjects, samples were taken from the bottom of the gingival crevice of proximal sites of the upper first molars.

### Isolation of bacteria

Samples were transported in tightly screw-capped vials and were transferred as soon as possible (within a few minutes) to an anaerobic glove box (Model AZ-Hard, Hirasawa, Tokyo, Japan) containing 80% $N_2$,

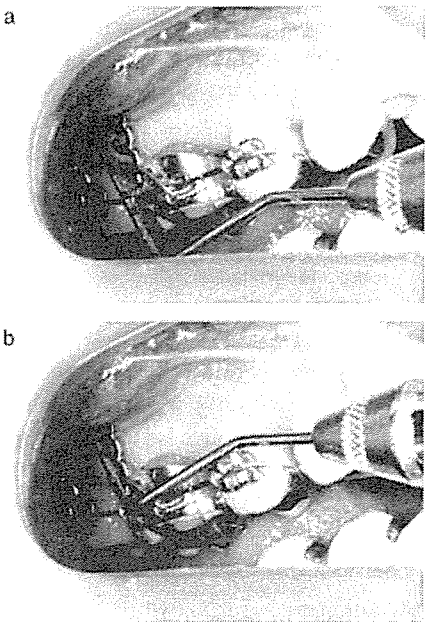


*Fig. 1.* Intraoral photograph of (a) an implanted titanium orthodontic anchor plate and (b) a periodontal pocket probe inserted into a transmucosal pocket.

***Table 1.*** **Clinical features of subjects in this study**

| | Healthy crevices with plates | | | | | | | | Inflamed crevices with plates | | | | Healthy gingival crevices (without plates) | | | | | | | |
|---|---|---|---|---|---|---|---|---|---|---|---|---|---|---|---|---|---|---|---|---|
| | 1 | 2 | 3 | 4 | 5 | 6 | 7 | Mean | 8 | 9 | 10 | Mean | 11 | 12 | 13 | 14 | 15 | 16 | 17 | Mean |
| Age | 24 | 23 | 25 | 20 | 20 | 29 | 25 | 23.7 | 24 | 25 | 23 | 24 | 23 | 25 | 24 | 26 | 24 | 26 | 25 | 24.7 |
| Gender | F | F | F | F | F | F | F | – | F | F | F | – | F | F | F | F | F | F | F | – |
| Loading periods* | 1.1 | 1.2 | 0.9 | 1.0 | 1.6 | 0.9 | 0.7 | 1.1 | 0.8 | 2.9 | 3.4 | 2.4† | – | – | – | – | – | – | – | – |
| Sampling periods‡ | 2.9 | 4.2 | 3.7 | 3.6 | 4.3 | 5.9 | 4.6 | 4.2 | 9.5 | 4.7 | 28.4 | 14.2 | – | – | – | – | – | – | – | – |
| Total implantation periods§ | 9.3 | 26.5 | 19.3 | 21.6 | 13.4 | 36.8 | 21.7 | 21.2 | 23.9 | 27.3 | 42.2 | 31.1 | – | – | – | – | – | – | – | – |
| Sampling site | R | R | L | R | L | L | R | – | L | L | L | – | R | L | L | R | L | L | R | – |
| Probing depths (mm) | 7 | 6 | 7 | 4 | 5 | 4 | 4 | 5.3¶ | 10 | 10 | 8 | 9.3¶,† | 3 | 2 | 2 | 2 | 2 | 2 | 2 | 2.1 |
| Plaque index | 1 | 0 | 0 | 0 | 1 | 0 | 0 | 0.3 | 3 | 1 | 0 | 1.3¶ | 0 | 0 | 0 | 0 | 0 | 0 | 0 | 0 |
| Gingival index | 1 | 0 | 0 | 1 | 1 | 0 | 1 | 0.6 | 4 | 2 | 2 | 2.7¶,† | 0 | 0 | 0 | 0 | 0 | 0 | 0 | 0 |

*Loading periods (months) by skeletal anchorage system.
†Significantly different ($P<0.05$) from the healthy crevices with plates.
‡Sampling periods (months) after implantation of titanium orthodontic anchor plates.
§Total implantation periods (months) after implantation of titanium orthodontic anchor plates.
¶Significantly different ($P<0.05$) from the healthy gingival crevices (without plates).
R and L indicate that samples were taken at the upper right and left molars sites, respectively.

10% $H_2$ and 10% $CO_2$. In the box each sample was suspended in 1 ml of sterilized 40 mM potassium phosphate buffer (pH 7) and dispersed with a teflon homogenizer. Serial 10-fold dilutions (0.1 ml each, from $10^{-4}$ to $10^{-6}$) were spread onto the surface of Fastidious Anaerobe Agar (FAA, Lab M, Bury, UK) plates (duplicate) supplemented with 5% rabbit blood (Nippon Bio-Test Laboratories, Tokyo, Japan) and incubated in the anaerobic glove box at 37°C for 7 days. All plates, media, buffer solutions and experimental instruments were kept in the anaerobic glove box for at least 24 h before use. To ensure strictly anaerobic conditions in the glove box, reduction of methylviologen (−446 mV) was carefully checked whenever the experimental procedures were carried out. After incubation for 7 days, all colonies from plates having fewer than 100 colonies were subcultured.

### Identification

#### Anaerobes and facultative anaerobes

Subcultured colonies were incubated anaerobically or aerobically for 3 days, and in this study, anaerobes were defined as bacteria which grew only in the anaerobic glove box, and facultative bacteria as those which also grew in air containing 30% $CO_2$, as described previously (Uematsu & Hoshino 1992; Sato et al. 1993).

#### DNA extraction and PCR-RFLP of 16S rRNA genes

Subcultured colonies were harvested by centrifugation at 7700 *g* for 5 min and the supernatants were removed. Genomic DNA was then extracted from the pellets with the InstaGene Matrix Kit (Bio-Rad Laboratories, Richmond, CA, USA) according to the manufacturer's instructions.

The 16S rRNA gene sequences were amplified by PCR using universal primers 27F and 1492R (Lane 1991) and Taq DNA polymerase (HotStarTaq Master Mix, Qiagen GmbH, Hilden, Germany) according to the manufacturer's instructions. The primer sequences were: 27F, 5′-AGA GTT TGA TCM TGG CTC AG-3′ and 1492R, 5′-TAC GGY TAC CTT GTT ACG ACTT-3′. Amplification proceeded using a PCR Thermal Cycler MP (TaKaRa Biomedicals, Ohtsu, Shiga, Japan) programmed as follows: 15 min at 95°C for initial heat activation and 35 cycles of 1 min at 94°C for denaturation, 1 min at 52°C for annealing, and 1.5 min at 72°C for extension and 10 min at 72°C for final extension. The 16S rRNA genes were individually digested with *Hpa*II or *Hae*III (New England Biolabs Inc., Ipswich, MA, USA) according to the manufacturer's instructions. Digestion products were separated on 2% agarose gels (High Strength Analytical Grade Agarose, Bio-Rad Laboratories) in Tris-borate EDTA buffer (100 mM Tris, 90 mM borate; 1 mM EDTA, pH 8.4), stained with ethidium bromide and photographed under UV light. The molecular size marker was a 100 bp DNA Ladder (Invitrogen Corp., Carlsbad, CA, USA).

#### 16S rRNA gene sequencing

Isolates were identified tentatively according to RFLP analysis (Sato et al. 1997, 1998a, 1998b, 2000, 2003; Sato & Kuramitsu 1999), and representative isolates were conclusively identified by sequence analysis as follows. The PCR products obtained above were sequenced at Hokkaido System Science Co. Ltd (Sapporo, Japan) using the BigDye Terminator Cycle Sequencing Kit and an automated DNA sequencer (PRISM-3100, Applied Biosystems Japan Ltd, Tokyo, Japan). Primers 27F and 1492R were used to sequence both strands (at least 1000 bp), and the partial 16S rRNA gene sequences were then compared with 16S rRNA gene sequences from the GenBank database using the Blast search program through the website of the National Center for Biotechnology Information. Bacterial species were determined by percent sequence similarity (>99%).

### Data analysis

Fisher's exact probability tests and Tukey's tests were used to analyze significance. *P* values of $<0.05$ were considered statistically significant.

## Results

Probing depths and gingival index of the inflamed anchor plate crevices were respectively greater than those of the healthy anchor plate crevices and healthy gingival crevices (Table 1). The plaque indices of the inflamed crevices were significantly greater than those of the healthy gingival crevices (Table 1). There were no significant differences in subject's age among the three crevices (Table 1). The average periods of loading by SAS were 1.1 and 2.4 months, sampling periods after implantation of titanium orthodontic anchor plates were 4.2 and 14.2 months, and total implantation periods after implantation of titanium orthodontic anchor plates were 21.2 and 31.1 months, in periodontally healthy subjects and inflammatory subjects, respectively. There were no significant differences in sampling and total implantation periods between the two groups, although the loading periods were longer in the inflammatory subjects than in the healthy subject (Table 1).

The average total colony-forming units (logarithm CFUs/ml) were 6.84 ± 0.85, 7.51 ± 0.76 and 8.88 ± 0.46 in healthy anchor plate crevices, inflamed anchor plate crevices, and healthy gingival crevices, respectively (Table 2), and significant differences were seen between healthy plate crevices and healthy gingival crevices, and between inflamed crevices and healthy gingival crevices. The amounts of bacteria were significantly lower in anchor plate crevices than in healthy gingival crevices (Table 2).

Table 2 shows the bacterial diversity in healthy and inflammatory anchor plate crevices and healthy gingival crevices. Of 184 strains isolated from healthy anchor plates crevices, 108 (59%) were anaerobic bacteria, while 73 (40%) were facultative bacteria. The predominant genera were *Actinomyces* (32 isolates, 17%), *Campylobacter* (22 isolates, 12%), *Fusobacterium* (19 isolates, 10%), *Selenomonas* (19 isolates, 10%) and *Streptococcus* (15 isolates, 8.2%). Of 133 strains isolated from inflamed anchor plate crevices, 110 (83%) were anaerobic and 17 (13%) were facultative bacteria. The predominant genera were *Prevotella* (62 isolates, 47%), *Fusobacterium* (22 isolates, 17%), *Campylobacter* (21 isolates, 16%) and *Eikenella* (10 isolates, 7.5%). On the other hand, of 146 strains isolated from healthy gingival crevices, 98 (67%) were facultative and 45 (31%) were anaerobic bacteria. The predominant genera were *Actinomyces* (54 isolates, 37%) and *Streptococcus* (29 isolates, 20%).

## Discussion

The amounts of bacteria in anchor plate crevices were significantly lower than in

***Table 2.*** **Bacterial isolates from crevices with orthodontic anchor plates and healthy gingival crevices**

| | Healthy crevices with plates | | | | | | | | Inflamed crevices with plates | | | | Healthy gingival crevices (without plates) | | | | | | | |
|---|---|---|---|---|---|---|---|---|---|---|---|---|---|---|---|---|---|---|---|---|
| | 1 | 2 | 3 | 4 | 5 | 6 | 7 | Total | 8 | 9 | 10 | Total | 11 | 12 | 13 | 14 | 15 | 16 | 17 | Total |
| Log (CFU/ml) | 7.84 | 6.34 | 5.81 | 6.81 | 7.85 | 5.94 | 7.31 | (6.84)*,† | 6.75 | 7.51 | 8.27 | (7.51)*,† | 9.23 | 9.41 | 8.15 | 8.45 | 8.74 | 9.20 | 8.98 | (8.88)* |
| Total of isolation | 16 | 29 | 25 | 14 | 29 | 18 | 53 | 184 | 92 | 16 | 25 | 133 | 22 | 24 | 16 | 22 | 19 | 20 | 23 | 146 |
| Anaerobes | 8 | 17 | 9 | 7 | 27 | 12 | 28 | 108 (59)‡ | 82 | 12 | 16 | 110 (83)† | 20 | 1 | 7 | 2 | 6 | 2 | 7 | 45 (31) |
| *Atopobium* | 1 | | | | | | | 1 (0.5) | | | | 0 | | | | | | | | 0 |
| *Campylobacter* | 1 | | 6 | 2 | 3 | 3 | 7 | 22 (12) | 3 | 3 | 15 | 21 (16) | | | 1 | | 1 | | 1 | 3 (2.1) |
| *Dialister* | 1 | | | | 4 | | 1 | 6 (3.3) | 2 | 1 | | 3 (2.3) | 1 | | | | | | | 1 (0.7) |
| *Fusobacterium* | 3 | | | 1 | 14 | 1 | | 19 (10) | 17 | 4 | 1 | 22 (17) | 1 | | | | | 1 | 2 | 4 (2.7) |
| *Leptotrichia* | | 8 | | 3 | | | 3 | 14 (7.6) | | | | 0 | | | | | | | | 0 |
| *Megasphaera* | | | | | | | | 0 | | | | 0 | | | | | | 1 | | 1 (0.7) |
| *Micromonas* | | | | | | | | 0 | | | | 0 | 2 | | 1 | | | | 1 | 4 (2.7) |
| *Mogibacterium* | 1 | | | | | | | 1 (0.5) | | | | 0 | 1 | | | | | | | 1 (0.7) |
| *Olsenella* | | | | | | | | 0 | | | | 0 | 9 | | | | | | | 9 (6.2) |
| *Peptostreptococcus* | | | | | | | | 0 | | | | 0 | 1 | | | | | | | 1 (0.7) |
| *Prevotella* | 1 | 4 | 1 | | 2 | 3 | 2 | 13 (7.1) | 59 | 3 | | 62 (47) | 5 | | | | 2 | | | 7 (4.8) |
| *Selenomonas* | | | | 1 | 4 | | 14 | 19 (10) | 1 | 1 | | 2 (1.5) | | 1 | | | | | 2 | 3 (2.1) |
| *Tannerella* | | | 2 | | | | | 2 (1.1) | | | | 0 | | | | | | | | 0 |
| *Veillonella* | | 5 | | | | 5 | 1 | 11 (6) | | | | 0 | | | 5 | 2 | 3 | | 1 | 11 (7.5) |
| Facultative anaerobes | 7 | 12 | 15 | 7 | 1 | 6 | 25 | 73 (40) | 7 | 4 | 6 | 17 (13)† | 2 | 22 | 9 | 19 | 13 | 17 | 16 | 98 (67) |
| *Actinomyces* | 4 | 2 | 4 | | | | 22 | 32 (17) | 2 | | 2 | 4 (3) | | 20 | 7 | | 12 | 1 | 14 | 54 (37) |
| *Capnocytophaga* | | 1 | | | | 1 | | 2 (1.1) | | | | 0 | | 1 | 1 | | | | 1 | 3 (2.1) |
| *Eikenella* | | | | 4 | | | | 4 (2.2) | 2 | 4 | 4 | 10 (7.5) | | | | | | | | 0 |
| *Gemella* | 1 | 1 | | | | | | 2 (1.1) | | | | 0 | | | | | | 3 | | 3 (2.1) |
| *Granulicatella* | | 1 | | | | | | 1 (0.5) | | | | 0 | | | | | | 1 | | 1 (0.7) |
| *Haemophilus* | | | 4 | | 1 | | | 5 (2.7) | | | | 0 | | 1 | | 1 | | | | 2 (1.4) |
| *Neisseria* | | | 7 | 3 | | 2 | | 12 (6.5) | | | | 0 | | | | 1 | | 2 | | 3 (2.1) |
| *Rothia* | | | | | | | | 0 | | | | 0 | | | | | 1 | 2 | | 3 (2.1) |
| *Streptococcus* | 2 | 7 | | | | 3 | 3 | 15 (8.2) | 3 | | | 3 (2.3) | 2 | | 1 | 17 | | 8 | 1 | 29 (20) |
| Unidentified | 1 | 0 | 1 | 0 | 1 | 0 | 0 | 3 (1.6) | 3 | 0 | 3 | 6 (4.5) | 0 | 1 | 0 | 1 | 0 | 1 | 0 | 3 (2.1) |

*Mean log (CFU/ml) are given in parentheses.

†Significantly different ($P<0.05$) from the healthy gingival crevices (without plates).

‡Percentages are given in parentheses.